Venus's shield terrain

Vicki L. Hansen[†]
Department of Geological Sciences, University of Minnesota, Duluth, Minnesota 55812, USA

ABSTRACT

Plains, planitiae, or lowlands—expanses of gentle, long-wavelength (~1000 km) basins—cover ~80% of Venus's surface. These regions are widely accepted as covered by volcanic flows, although the mechanism(s) responsible for resurfacing remains elusive; in addition, a volcanic origin for the lowland surface may be open to question. Lowland resurfacing is typically attributed to catastrophic emplacement (10–100 m.y.) of globally extensive, thick (1–3 km) flood-type lava. This model of resurfacing has been postulated on the basis of impact crater distribution, taken together with a lack of obvious volcanic flows or edifices, and a lack of viable alternative models. Ongoing geologic mapping of ~15,000,000 km² (0–25N/90–150E) using 225 m/pixel and 75 m/pixel NASA *Magellan* SAR (synthetic aperture radar) data indicates that small edifices, called shields (1–15-km-diameter edifices, <<1 km high), play a major role in lowland resurfacing. Individual shields are radar-smooth or -rough, quasi-circular to circular features with or without a central pit. Shield shapes, which have been previously documented, range from shield, dome, or cone, to flat-topped or flat. Shield deposits typically coalesce, forming a thin, regionally extensive but discontinuous, mechanically strong layer, herein called shield paint. Shield paint conforms to delicate local topography, providing evidence of its thin character and indicating generally low viscosity during emplacement. Shield terrain (shields and shield paint) covers more than 10,000,000 km² within the study area. Detailed mapping of five 2° × 2° regions using coregistered normal and inverted right- and left-illumination SAR imagery indicates shield densities of 3500–33,500 shields/10⁶ km²; thus, the map area hosts more than 35,000–335,000 shields. Shield terrain generally postdates, but is also locally deformed by, fractures and wrinkle ridges, indicating time-transgressive formation relative to local deformation and/or reactivation. The regional scale crust was strong throughout shield-terrain formation. Shield terrain may extend across much of Venus's surface.

Keywords: Venus, shields, resurfacing, flood lava, mud volcano, partial melt.

INTRODUCTION

Understanding processes that affect Venus's lowlands is critical to Venus evolution models. Lowlands—expanses of gentle, long-wavelength topography at or below 1.5 km mean planetary radius—cover ~80% of Venus (Masursky et al., 1980). Although lowland materials are widely considered volcanic (Banerdt et al., 1997), the mechanism(s) responsible for lowland volcanism remain mostly elusive. Lowland resurfacing is typically attributed to emplacement of extensive flood lava (e.g., Banerdt et al., 1997). This supposition forms the basis for two related hypotheses: catastrophic resurfacing (Strom et al., 1994) and global stratigraphy (Basilevsky and Head, 1996, 1998, 2002; Head and Basilevsky, 1998). The related hypotheses imply that Venus's lowland was covered very quickly (<10–100 m.y.) by thick (1–3 km) flood-type lava ca. 750 +350/–400 Ma (global average model surface age [McKinnon et al., 1997]). Such thick layers of lava are postulated in order to account for complete burial of preexisting impact craters that are presumed to have formed on tessera terrain and fracture terrain that, within the context of the hypothesis, form globally extensive basement units. Impact crater rim-to-trough heights range from 0.2 to 1.5 km (Herrick and Sharpton, 2000), thus requiring a flood-lava thickness greater than 1.5 km to cover early-formed craters. The global stratigraphy hypothesis implies that "wrinkle-ridge plains" or "regional plains" represent the catastrophically emplaced, globally extensive flood lava that buried all preexisting impact craters across Venus's lowland. But currently no robust temporal constraints are available with regard to the emplacement rate of Venus surfaces, whether punctuated, catastrophic, or continuous (Campbell, 1999). In addition, no studies explicitly evaluate a flood-lava mechanism for lowland resurfacing. The flood-lava hypothesis has been accepted because of a lack of obvious volcanic flows or edifices, or because alternative viable models exist. Thus, it is important to determine the range of sources and the types of processes that contributed to lowland resurfacing.

Locally, coronae, circular to quasi-circular tectonomagmatic features that range in size from ~60 to 1000 km in diameter (200-km mean; Stofan et al., 1992), expelled lava flows that extend over 500 km and locally contribute lava to adjacent lowlands (e.g., Chapman, 1999; Rosenberg and McGill, 2001; Campbell and Rogers, 2002; Hansen and DeShon, 2002; Young and Hansen, 2003). However, many lowlands, including those in the Niobe-Greenaway (0–25°N/90–150°E) area, lack adjacent coronae or coronae-source lava flows. This contribution examines the extensive tract of Venus's lowland in the Niobe-Greenaway area (Figs. 1 and 2) in order to expressly evaluate lowland surface processes.

The results reveal no evidence for widespread flood-lava flows; rather, tens to hundreds of thousands of small eruptive centers dominate the lowland across over 10,000,000 km². Individual eruptive centers (shields) and associated deposits that coalesce into an extensive, thin, mechanically strong layer (shield paint) together form shield terrain. Shield terrain formed in a time-transgressive manner and is cut by distributed low-strain deformation marked by extension fractures, wrinkle ridges, and inversion structures. Shield-terrain evolution seems inconsistent with the catastrophic flood-lava resurfacing hypothesis. Possible models for shield-terrain formation include widespread sedimentation and mud volcano formation, and shallow in situ point-source partial-melt formation resulting in tertiary melt that subsequently rises to the surface along preexisting fractures. Both of these hypotheses present quite different pictures of ancient Venus compared with contemporary Venus.
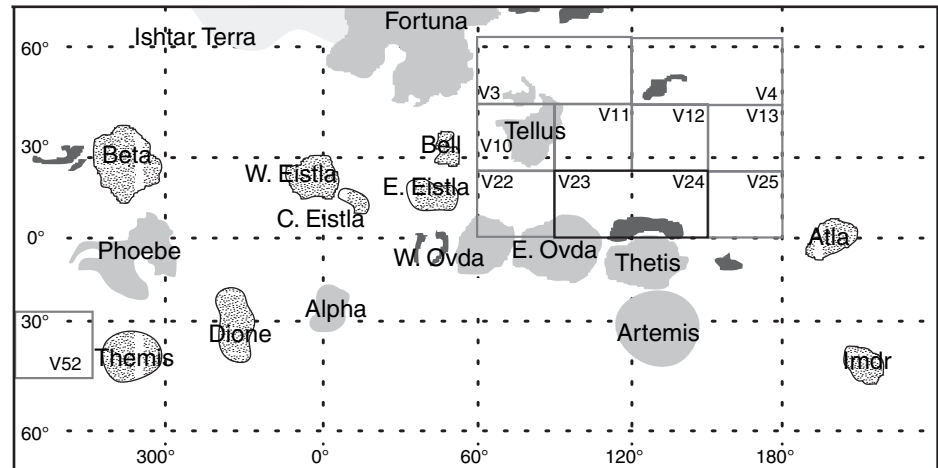
BACKGROUND

Venus's Geology

Venus exhibits three global topographic provinces—lowlands, mesolands, and highlands—

[†]E-mail: vhansen@d.umn.edu.

and several types of geomorphic features (Phillips and Hansen, 1994). The lowlands (~80% of the surface at or below mean planetary radius, ~6052 km) are relatively smooth, with widely distributed low-strain deformation and belts of concentrated deformation (Banerdt et al., 1997). Highlands (<10% of the surface, ~2–11 km above mean planetary radius) include: (1) volcanic rises—huge (~1100–1800 km diameter) domical rises dominated by volcanic features and analogous to terrestrial hot spot rises (Smrekar et al., 1997); (2) crustal plateaus—huge (~1400–2300 km diameter) quasi-circular plateaus characterized by deformed crust and supported by thicker than average crust; and (3) Ishtar Terra, a globally unique feature in the northern hemisphere (Hansen et al., 1997, and references therein). About 500 coronae (~60–1000-km-diameter quasi-circular tectonomagmatic features) and spatially associated chasmata (troughs) are concentrated in the mesoland, although coronae clusters associate with some volcanic rises, and isolated coronae occur in the lowlands (Stofan et al., 1992, 1997, 2001).

Venus preserves a range of volcanic features, many dwarfing similar terrestrial features. Large volcanic edifices range up to hundreds of kilometers in diameter, and lava flows can extend for hundreds of kilometers (Head et al., 1992; Crumpler et al., 1997). Venus also preserves very small features (<1–15 km diameter) called shields, interpreted as volcanic in origin (Aubele and Slyuta, 1990; Guest et al., 1992; Head et al., 1992; Crumpler et al., 1997). Shields are divided into two morphological terrains on the basis of regional extent: shield clusters and shield plains (Crumpler et al., 1997). Shield clusters (or shield fields) comprise groups of shields distributed over quasi-circular regions ~50–350 km in diameter (100–150-km-diameter mode); shield plains (Aubele, 1996) consist of ~4500 shields/10^6 km^2 over millions of square kilometers. Fluid-cut channels, extending tens to hundreds of kilometers up to the ~6900-km-long Baltis Vallis, trace across the surface (Baker et al., 1997). The channels are typically narrow (several kilometers), shallow (tens of meters), and curved to sinuous, with little change in width and depth along their length.

The entire surface of Venus is broadly accepted as basaltic composition, a finding based in part on Venera data, as well as on theoretical arguments (e.g., Banerdt et al. 1997; Grimm and Hess, 1997). Each of the volcanic forms is consistent with basaltic composition (Bridges, 1995, 1997; Stofan et al., 2000), although the many unknowns inherent in planetary geology leave the door open for other possibilities, including the prospect that some features are fluvial rather than volcanic (e.g., Jones and Pickering, 2003).

Figure 1. Distribution of Venusian features. Fine dots, volcanic rises; dark areas, large ribbon terrain; light gray areas, crustal plateaus (modified from Hansen et al., 1999). The map area (Fig. 2) includes V23 and V24; the V labels show the locations of other map quadrangles discussed in the text.

About 970 essentially pristine impact craters (2–270 km diameter) display a near spatially random distribution (Phillips et al., 1992; Schaber at al., 1992; Herrick et al., 1997; Hauck et al., 1998), reflecting a global average model surface age of ca. 750 +350/–400 Ma (McKinnon et al., 1997). Interpretation of global average model surface age is nonunique. Many plausible surface histories are possible, including: (1) catastrophic resurfacing at t = average model surface age; (2) 50% of surface formed at $0.5t$ and 50% at $1.5t$; or (3) 20% of surface formed at $2t$ and 80% at $0.75t$). Average model surface age also refers to pristine impact craters, so if other impact crater forms exist that have not yet been recognized, then the model age value will change (Hansen and Young, 2004). Although the average model surface age can accommodate a range of surface histories, Venus apparently lacks large (>20,000,00 km^2) coherent tracts of young or old surface crust, as evidenced by impact crater distribution (Phillips et al., 1992; Phillips, 1993).

Venus's Environment

Venus's surface conditions are intimately related to its atmospheric properties. Currently, its caustic dense atmosphere (92 bars; 0.96 CO_2, 0.035 N, and 0.005 H_2O, H_2SO_4, HCl, and HF), includes three cloud layers from ~48 to 70 km above the surface that reflect visible light, blocking optical observation (Donahue et al., 1997). Although Venus is presently ultradry, it is quite possible that water existed on the planet in the past. Isotopic data are consistent with an extensive water reservoir ≥1 billion years ago (Donahue et al., 1982; Donahue and Russell,

1997; Donahue, 1999; Hunten, 2002). In addition, a comparison of carbon, nitrogen, and water abundances at the surface of Earth and Venus indicates that both planets likely had similar primitive atmospheres that reacted differently with their surfaces. For Venus, the rate of water loss would affect deuterium/hydrogen ratios (Donahue and Russell, 1997). In addition, a combination of crustal hydration and hydrogen-escape processes could explain the present-day low amount and high deuterium/hydrogen ratio of water in the Venusian atmosphere (Lecuyer et al., 2000). Lecuyer et al. (2000) further argue that if Venus's high deuterium/hydrogen ratio resulted from hydrogen escape alone, then the reservoir of remaining oxygen would require crustal oxidation to a depth of ~50 km. Hydrated basalt is considered further below.

Venus climate models also indicate that ancient surface temperatures could have reached or exceeded 1000 K as a result of a high level of greenhouse gases (Bullock and Grinspoon, 1996, 2001; Phillips and Hansen, 1998; Phillips et al., 2001). These ancient environmental conditions could have lead to the loss of large water reservoirs with time (e.g., Bullock and Grinspoon, 1996, 2001). Therefore, Venus could have been both significantly wetter and hotter in the past.

The current lack of water renders contemporary Venusian crustal rock orders of magnitude stronger than terrestrial counterparts, even given Venus's elevated surface temperature (Mackwell et al., 1998); again, the crust may not have been this strong in the past if ancient Venus was wetter or hotter, or both.

Globally, Venus appears to be composed of basaltic crust, an interpretation supported in part

Figure 2. Generalized geologic map of V23 and V24 quadrangles, Venus. Units: medium gray, basal ribbon terrain; medium dark gray, basal fracture terrain; white, shield terrain; lightest gray, volcanic flows associated with medium-size volcanoes or coronae; dark gray, impact crater deposits. Primary structures: gray lines with arrows, flow directions. Tectonic lineaments: thin gray lines (generally trend E–W), wrinkle ridges; thin black lines, fractures; medium-weight gray lines, folds; thick dark gray lines, broad ridges. Locations of Figures 3A and 3B are indicated; numbered boxes show locations of Figures 4–8. Box shown in dashed line indicates the areal extent of the entire Snake River Plain and Columbia River Plateau basalt provinces of the northwestern United States. See text for discussion.

by *Magellan* hypsometry (elevation referred to mean planetary radius) that indicates unimodal versus terrestrial bimodal (oceans and continents) distribution of surface elevation (Pettengill et al., 1980; Ford and Pettengill, 1992; Grimm and Hess, 1997). However, although hypsometry seems to indicate that Venus lacks large tracts of felsic and mafic crust like the Earth's oceans and continents, the data do not require a complete lack of crustal differentiation. The hypsometric data can limit the spatial scale of differentiation. But the hypsometric data alone cannot resolve small-scale crustal density differences or differences in density that might occur in crustal layers. For example, if Venus's crust were layered with felsic and mafic components, it could have unimodal rather than bimodal hyposometry. Thus, the data, which show unimodal hyposometry, can be met by a multitude of crustal models.

Given the current nascent stage of our understanding of Earth's sister planet, it is perhaps best to consider the broadest range of possible environmental conditions and gross planet architecture in working hypotheses.

NIOBE-GREENAWAY MAP AREA

The map area (0–25N/90–150E), which includes ~10,000,000 km^2 of lowlands, is bounded to the south by crustal plateaus Ovda and Thetis regions, and to the west, north, and east by planitiae (Fig. 1). The map area includes Niobe, Sogolon, and Llorona planitiae, eastern Ovda Regio, and Haasttse-baad and Gegutte tesserae (Fig. 2). The division between Niobe and Sogolon planitiae is generally topographic, with Sogolon comprising a relatively small, circular basin; Gegutte Tessera separates Niobe and Llorona planitiae. Niobe and Llorona planitiae are centered northwest and northeast of the study area, respectively. Llorona Planitia is divided by a N-trending broad topographic rise marked by a chain of coronae (Fig. 2). The area includes several other coronae, but only Rosmerta Corona, which cuts Haasttse-baad Tessera, shows well-developed radial fractures and extensive flows. The other coronae are similar to "old" coronae of Chapman and Zimbelman (1998), defined by low circular basins with raised rims and concentric fractures, and generally lacking obvious radial fractures or extensive volcanic flows. Volcanic flows from Ituana Corona, east of the study area (which, like Rosmerta, is similar to "young" coronae of Chapman and Zimbelman [1998]), flood part of Llorona Planitia in the northeast; to the east, northeast, and southeast of the study area, "young" corona-sourced flows contribute to resurfacing of Rusalka and Llorona planitiae (DeShon et al., 2000; Hansen and

DeShon, 2002; Young and Hansen, 2003). The map area hosts ~50 pristine impact craters.

Regions shaped by deformation include ribbon tessera terrain (or ribbon terrain) and fracture terrain. Ribbon terrain, marked by a unique parallel ridge and trough deformation fabric, is inferred to record the signatures of deep mantle plumes on ancient thin Venusian lithosphere (e.g., Hansen and Willis, 1998; Phillips and Hansen, 1998; Hansen et al., 1999; Ghent and Tibuleac, 2002). (For a discussion of ribbon-terrain controversies, see Gilmore et al. [1998] and Hansen et al. [2000].) Fracture-terrain hosts penetratively developed (i.e., spaced to image resolution) parallel fractures. The relative age of ribbon- and fracture-terrain deformations is unconstrained. Structural trends within small isolated kipukas of ribbon terrain and fracture terrain describe regionally coherent patterns with larger tracts of these terrains. This observation is consistent with the interpretation that these terrains extend as local "basement" between isolated kipukas, as initially proposed by Ivanov and Head (1996), although the basal terrain need not be globally distributed, as originally suggested.

Materials that locally postdate ribbon and penetrative fracture formation variably cover the map area. Cover materials are cut by E- to ENE-trending contractional wrinkle ridges, and variably preserved N- to NNW-striking (extension) fractures that display regionally coherent patterns across the map area (Fig. 2). Locally preserved concentric ridges may mark "old" coronae structures.

Reconnaissance regional mapping and local detailed mapping do not reveal obvious evidence of emplacement of thick massive flood-type lava flows; instead, shield plains (e.g., Aubele, 1996) appear to cover much of the lowland. Local lobate flow boundaries and primary flow structures record paleoflow direction from centralized locations, but much of the region lacks any indication of flow directions, even in full-resolution SAR (synthetic aperture radar) data. Full-resolution SAR imagery shows thousands of shields that decorate the lowland. The occurrence of numerous small, isolated ribbon-terrain kipukas across much of the study area indicate that surface deposits are thin and that basal material lies at shallow depths across much of the region (Hansen, 2002; Lang and Hansen, 2003). Aubele (1996) briefly described shield plains, but no study has investigated shield-plains formation. This study focuses on understanding shield-plains formation.

Terminology

Although this work concerns the evolution and formation of "shield plains" (as opposed to shield clusters), the term "shield terrain" is used herein because the descriptor "plains" carries several nonunique connotations. It is useful to clarify the terms used herein because in many cases, terminology carries stated and unstated assumptions with regard to genetic implications.

Some workers lump Venus's lowland units together as "regional plains" or "wrinkle-ridge plains" (e.g., Johnson et al., 1999; McGill, 2000; Rosenberg and McGill, 2001; Campbell and Rogers, 2002; Ivanov and Head, 2001a). Some workers also describe a wide range of plains units, including smooth, lineated, densely lineated, fractured, densely fractured, mottled, lobate, homogeneous, inhomogeneous, wrinkle-ridged, and shield plains (e.g., Basilevsky and Head, 1996, 1998, 2002; Head and Basilevsky, 1998; Johnson et al., 1999; McGill, 2000; Rosenberg and McGill, 2001; Ivanov and Head, 2001b; Campbell and Rogers, 2002). These terms are commonly confusing for three reasons: (1) "Plains" refers to geomorphology rather than a geological material; "regional plains" presumably cover large flat areas; but large, flat areas could host several map units. (2) The terms "lineated," "fractured," "wrinkled," "ridged," etc., suggest that secondary structures (lineations, fractures, wrinkle ridges) define individual plains units; this violates fundamental geologic mapping practice, and it confuses delineation of geologic history because it disallows temporal distinction between unit emplacement and unit deformation (Tanaka et al., 1994; Hansen, 2000; McGill, 2004). (3) Many workers assume that regional and wrinkle-ridge plains represent extensive flood-type lava that emerged catastrophically across the planet (e.g., Basilevsky et al., 1997; Head and Coffin, 1997; Basilevsky and Head, 1998, 2002; Head and Basilevsky, 1998); yet there is no robust evidence that material was emplaced as flood lava, that volcanic products share an origin resulting from widespread melting of the mantle, as presumed for terrestrial flood lava, or that lava was emplaced quickly. Thus, these terms confuse geomorphic and geologic unit terminology; intertwine unit emplacement and unit deformation; may imply genetic source(s); and may lead to unstated or unsupported inferences with regard to emplacement rates. Each of these problems, individually and collectively, confuses the goal of geologic mapping, which is to determine the geologic history of a region with the express goal of understanding formational processes (e.g., Gilbert, 1886; Tanaka et al., 1994; Hansen, 2000).

For clarity, the term "lowland" is used in a topographic sense in reference to broad regional long-wavelength basins. Planitia (singular) or planitiae (plural), used in a geomorphic sense, refers to individual basins or lowland regions (e.g., Niobe and Sogolon planitiae). The term "plains" is used to describe geologic units only in reference to published work. Every attempt is made to clearly separate secondary structures from material units. Locations, orientations, and relative densities of primary (e.g., shield edifices, flow indicators) and secondary structures (e.g., fractures, wrinkle ridges) are shown independent of material units.
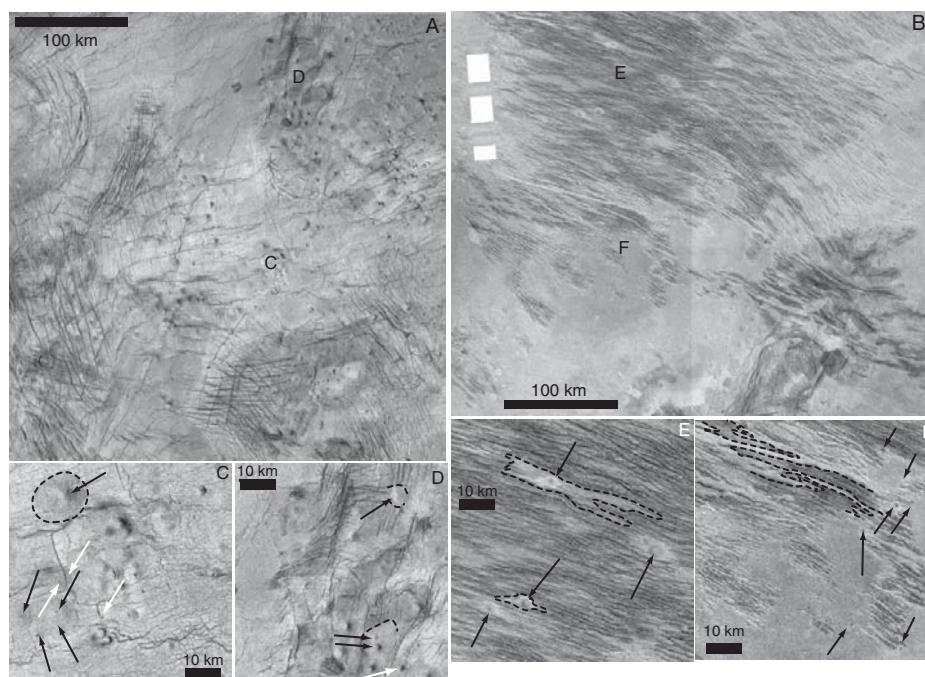
The term "terrain" describes a texturally defined region. Characteristic texture could imply a shared history, similar to terrestrial "gneissic terrain" used to describe a particular shared history, such as a tectonothermal history or event, responsible for melding possibly previously unrelated rock units (any combination of igneous, metamorphic, and sedimentary rocks) into a new package. As with gneissic terrain, there is no implication of a unique history *prior to* the event(s) that melded potentially separate units into the textural terrain. Events prior to terrain formation would be unconstrained unless specifically noted. Examples of terrain in this study include ribbon tessera terrain (or ribbon terrain), fracture terrain, and shield terrain.

Shield terrain differs from ribbon and fracture terrain in that it comprises rocks with shared emplacement mechanism (represented by primary structures), as opposed to shared deformation history (represented by secondary structures). Shield terrain would be comparable, for example, to a terrestrial sedimentary formation composed of turbidite deposits from multiple source regions. In the case of shield terrain, we have little knowledge of the absolute time involved in terrain formation, whereas a terrestrial turbidite terrain might have many accessible clues with regard to temporal evolution. Thus, Venusian shields are classified as belonging to either localized shield clusters (distributed across areas ~50–350 km in diameter; 100–150-km mode-sized regions) or regionally extensive shield terrain (millions of square kilometers); shield terrain is the focus of the current contribution. Shield terrain includes edifices (shields) and associated deposits (shield paint), as described further below.

Data and Methodology

The work here emerged from regional reconnaissance and locally detailed geologic mapping that used NASA *Magellan* S-band SAR and altimetry data. Data included: (1) compressed "C1" (~225 m/pixel) SAR data, (2) synthetic stereo imagery constructed following the method of Kirk et al. (1992) using NIH-Image macros developed by D.A. Young, (3) *Magellan* altimetry (~8 km along-track by 20 km across-track footprint with ~30-m average vertical accuracy

Figure 3. Inverted right-illumination SAR images; (A) and (B) cropped from C1 SAR images (locations in Fig. 2); detail images (C–E) are cropped from full-resolution SAR (locations in [A] and [B]). (A) Image detail of tectonic structures and shields. Concentric structures in the upper left are part of Maya Corona that dominantly predates shield-terrain formation; NNW-striking fractures and ENE-trending wrinkle ridges parallel regionally extensive suites. E-striking fractures in the bottom of the image occur within a more localized region (see Fig. 2). Shields pepper the surface. Enlargements (C) and (D) show a range of shield morphologies and temporal relations with secondary structures. Black arrows point to a few shields from well to poorly defined. N-striking regional fractures generally predate shield formation and reactivation along N-striking fractures locally postdates shield emplacement (white arrows); dashed lines indicate examples of well-defined limits of shield deposits (upper D) and more poorly defined limits (C and lower D); local regions of basal fracture terrain are exposed as kipukas among shield deposits (D). (B) Shield deposits coalesce to form a discontinuous layer that variably covers basal fracture terrain marked by extremely closely spaced WNW-striking fractures. Enlargements (E) and (F) show detailed relations: locally isolated shield deposits are completely surrounded by older fracture terrain (local contacts marked by dashed line) and shield deposits preferentially fill subtle lows ([F] in particular); arrows mark locally well-defined shields; eruptive centers can be difficult to identify. Minor reactivation of fractures may cut the thinner distal part of individual shield deposits (E); individual shield deposits locally coalesce forming an extremely thin layer that blankets earlier tectonic fabrics (F). Detail of the boundary between basal fracture terrain and shield paint, including the occurrence of shield deposits as islands (E), indicates the shield-paint layer is extremely thin.

which improves to ~10 m in smooth areas [Ford and Pettengill, 1992; Ford et al., 1993]), and (4) full-resolution "F" (75–100 m/pixel) SAR imagery of both right- and left-illumination data. All images (F, C1, and synthetic stereo) were viewed in both normal and inverted (negative) modes to highlight details of primary and secondary structures; lineaments are typically more apparent in inverted images. All images presented herein are inverted and right-illuminated unless noted. In inverted SAR images, radar-smooth areas appear bright and radar-rough areas appear dark. In addition, apparent illumination is reversed; hence, right-illuminated inverted images appear left-illuminated. Five 2° × 2° areas were mapped by four full-resolution SAR images of the same region: right and left illumination, and normal and inverted. Images were coregistered on the basis of fractures and wrinkle ridges—features that should be relatively unaffected by radar artifacts in near equatorial locations. *Magellan* SAR imagery is available at http://pdsmaps.wr.usgs.gov/maps.html. SAR interpretation follows Ford et al. (1993); map-

ping follows guidelines and cautions of Wilhelms (1990), Tanaka et al. (1994), and Hansen (2000).
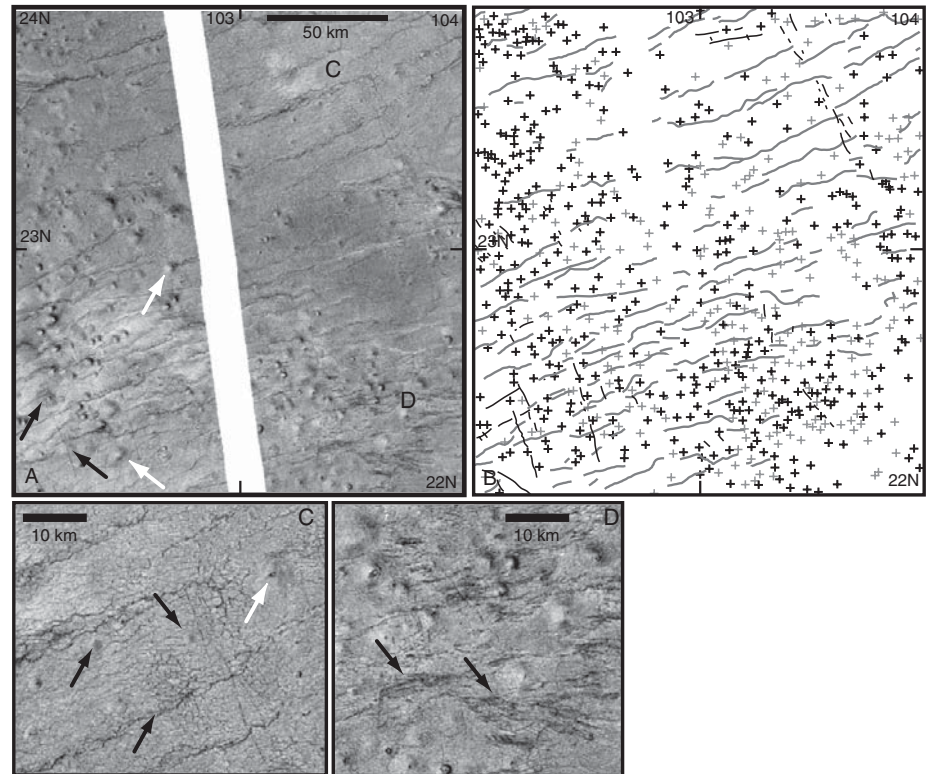
Shield Terrain

Shields across the study area, like those previously described in detail (e.g., Guest et al., 1992), are small (<1–15 km diameter), quasi-circular to circular, radar-dark or radar-bright features with or without topographic expression (with shapes ranging from shield, dome, cone, flat-topped, or flat), and with or without a central pit (Fig. 3). The smallest size of preserved shield edifices is difficult to determine given that many pixels are needed to image a single shield; thus, although *Magellan* SAR data has ~100 m/pixel resolution, the effective resolution for shield size is likely ~0.5–1 km in diameter (e.g., Masursky et al., 1970; Guest et al., 1992; Zimbelman, 2001). Minimum discernible shield diameter depends on size, morphology (e.g., steep-sided shields imaged better), radar incidence angle, radar contrast with surroundings, texture of surroundings, and character and number of adjacent shields. Given that ~0.5–1-km-diameter shields, essentially effective image-shield resolution, can be identified locally, it is likely that even smaller shields occur within the study area. Guest et al. (1992) reached a similar conclusion. Given the range of shield size and morphology relative to data resolution, the experience of an individual mapper also comes into play in shield identification. In addition to the factors noted above, shield size is difficult to constrain because shield bases are commonly poorly defined; individual edifices typically appear to blend smoothly into a base layer composed of coalesced shield deposits (Fig. 3C). In some cases, a slight difference in radar backscatter or truncation of preexisting underlying structural fabric can define the apparent limit of individual shield deposits, or it might mark a change in thickness of shield deposit material (Fig. 3D). Figure 3 illustrates a range of shield morphologies: (1) aprons that blend outward into surrounding terrain, (2) edifices in marked distinction from surroundings (Fig. 3A), (3) edifice morphologies from steep to broad, cone-shaped to flat-topped, and (4) extremely flat regions in which material flowed as low-viscosity material into the lows of delicate topography (Fig. 3E), forming smooth local surfaces (Fig. 3F).

Embayment relations indicate that shield deposits seem to have flowed across the surface and into local topographic lows and around local topographic obstacles; in addition, material from adjacent edifices seems to coalesce into a thin layer (Figs. 3E, F). The layer apparently acquired strength after emplacement (Figs. 3A,

C, D, and below). I refer to the nonedifice deposits as "shield paint" because of inferred low viscosity during emplacement (like liquid paint), apparent coalescing of adjacent deposits, and acquisition of postemplacement mechanical strength (like dry paint). Shield paint forms a thin deposit that could be formed from any combination of lava flows, air-fall deposits, or pyroclastic flows. Guest et al. (1992) reached a similar conclusion. Shield paint forms a thin, locally discontinuous layer that is lace-like in appearance; shield paint locally hides, and thinly veils, stratigraphically lower, fracture terrain (Fig. 3). The scale of lacy holes in the shield-paint veil ranges from hundreds to tens of kilometers, to the resolution of the SAR imagery. To clarify, "shield" refers to individual edifices; "shield paint" refers to material interpreted to have emerged from the edifices and that locally surrounds edifices forming a coherent (mechanical) layer; and "shield terrain" refers collectively to shields and shield paint. Shields are primary structures, shield paint is a composite deposit, and shield terrain the composite map unit that displays a characteristic texture.

Shield terrain displays a range of temporal relations with local materials and/or structures. For example, shield-terrain formation postdates the major formation of Maya Corona preserved in the NW image area (Figs. 2 and 3A). Although local reactivation of concentric fractures associated with Maya occurred after some shield-paint formation, as indicated by crosscutting relations. Evidence of structural reactivation following shield-paint emplacement is common across the study area. Wrinkle ridges also deform shield paint (Fig. 3A).

The pattern of shields and preexisting tectonic fabric in southern Llorona Planitia illustrates the detailed spatial nature of the contact between older basal fracture terrain and younger overlying shield terrain (Figs. 2 and 3B). In the region dominated by fracture terrain, shields locally mask the delicate structural fabric (Fig. 3E). In the region dominated by shield terrain, shield paint forms a smooth, continuous layer; individual shields can be difficult to delineate, although interactive image stretching reveals a few local edifices. In this region, the contact between fracture terrain and shield terrain is extremely digitate at a local scale because shield paint follows local fracture-related topography (Fig. 3F). Regionally, the contact is gradational across ~150 km; few obvious shields occur at location (E) in Figure 3B, and the surface becomes shield dominated, with only local preservation of basal fracture terrain, at the eastern edge of Figure 3B. This region generally resides below a 6051.5-km radius, with very low topographic relief across the region. (Note

Figure 4. Area 23N/103E; right-illuminated inverted SAR (A) and geologic map (B) highlighting definite shields (black crosses), potential shields (gray crosses), wrinkle ridges (gray lines), and fractures (black lines); white indicates regions of shield terrain. Locations of enlargements (C) and (D) are indicated. The geologic map (B) was constructed by using coregistered right- and left-illumination SAR in both normal and inverted modes (as a result, the map does not show the data gap in shields that shows up in [A], the right illumination image). Relative spacing of wrinkle ridges and shields results in inconclusive temporal relations (A and C); although some shields postdate secondary structures (white arrows), in most cases shields are older than wrinkle ridges or fractures (black arrows), indicating wrinkle ridges dominantly postdate shields. Fine-scale polygonal fabric occurs between wrinkle ridges and is best developed away from shield centers where the unit is likely thin (C). (D) Primary shield structures locally cover, and therefore formed after, locally preserved basal layer marked by closely spaced E-trending anastomosing lineaments (black arrows).

that fracture terrain is considered "basement" to the catastrophically emplaced flood lava in the global stratigraphic hypothesis.) The extremely complex contact between underlying fracture terrain and shield terrain across such an extensive low-relief area indicates that shield paint is very thin. This interpretation is consistent with the estimate of Guest et al. (1992) that shield-associated deposits are likely tens of meters or less in thickness. Robust quantification of layer thickness is difficult with available SAR data, but tens of meters or less is consistent with the lace-like character of shield paint.
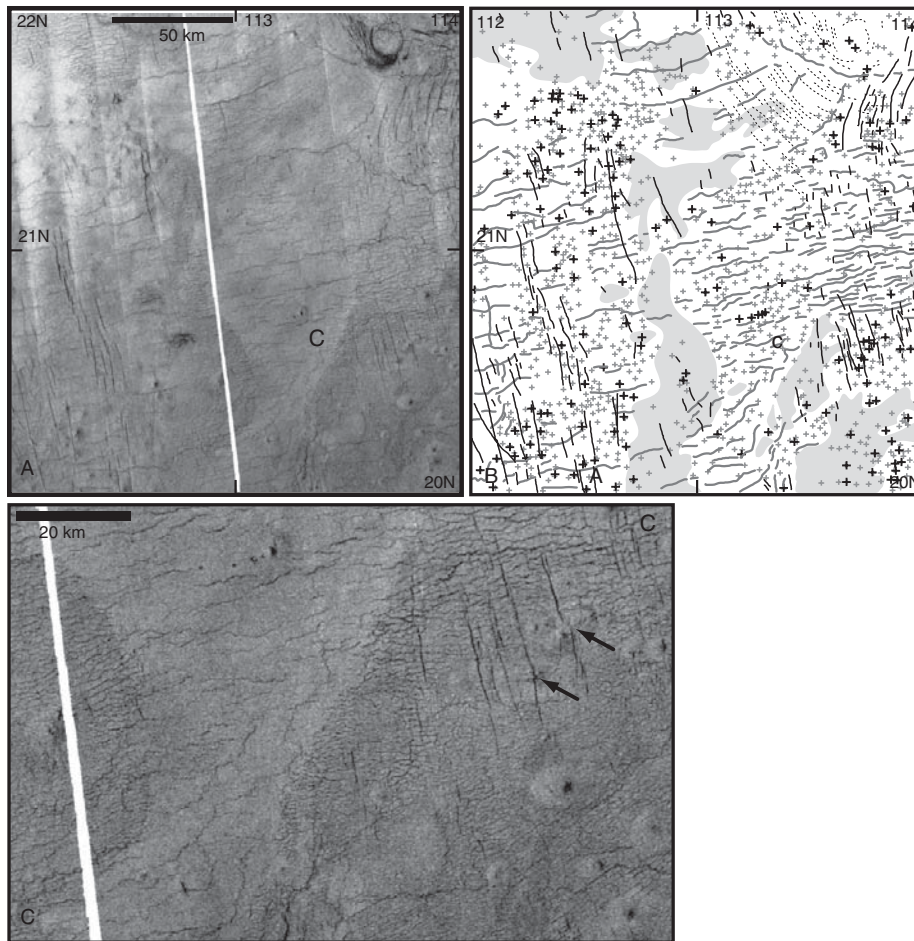
Any model of resurfacing for Niobe, Sogolon, or Llorona planitiae must consider formation of shield terrain. Critical constraints for any hypothesis include the extent of shield terrain,

shield patterns, shield density, and temporal relations with adjacent units or structures. Geologic mapping with C1 SAR data did not reveal any shield patterns. Shields do not appear to cluster, but rather they occur across the lowland; as such, shields fit the description of shield terrain (shield plains of Aubele [1996]). Southern Llorona Planitia shield terrain shows little to no evidence of reactivation of underlying structures following shield-terrain emplacement.

Detailed Mapping

Detailed geologic maps of five 2° × 2° areas were constructed to examine local shield patterns, densities, and relations with ribbon terrain and secondary structures (Figs. 4–8). Each

VENUS'S SHIELD TERRAIN

Figure 5. Area 21N/113E; right-illuminated inverted SAR (A) and geologic map (B); symbols as in Figure 4; location of enlargement (C) shown in (A) and (B). Wrinkle ridges trend ENE; fractures strike NNW. Well-developed fine-scale polygonal fabric occurs in patches (light gray). The boundary between regions displaying fine-scale polygonal fabric and regions lacking fine-scale fabric is sharp to gradational (C), and may reflect the relative thickness of shield paint with fine-scale polygonal fabric marking thinner shield paint. NNW-striking open fractures that locally cut shields and shield paint (C, arrows) likely represent reactivation of regional NNW-striking fractures. An ~15-km-diameter circular depression marks the NE corner of the area; extremely fine, typically covered, fractures concentric to this structure extend ~60–70 km from its center (dotted lines).

most definite shields; 13N/111E has the fewest definite shields and the most combined shields. The average number of definite shields and combined shields across all five areas is 247 and 938, respectively, representing average total densities of ~6255 and ~23,445 shields/10^6 km^2, or ~62,500–281,330 shields across 10,000,000–12,000,000 km^2. This shield density is slightly greater than Aubele's (1996) shield plains (4500 shields/10^6 km^2), but quite comparable considering the factors related to shield identification noted above.

Each map region hosts regional E- to ENE-trending wrinkle ridges and N- to NNW-striking fractures (Figs. 2 and 4–8). Each map area yields clues for shield-terrain formation, as discussed below.
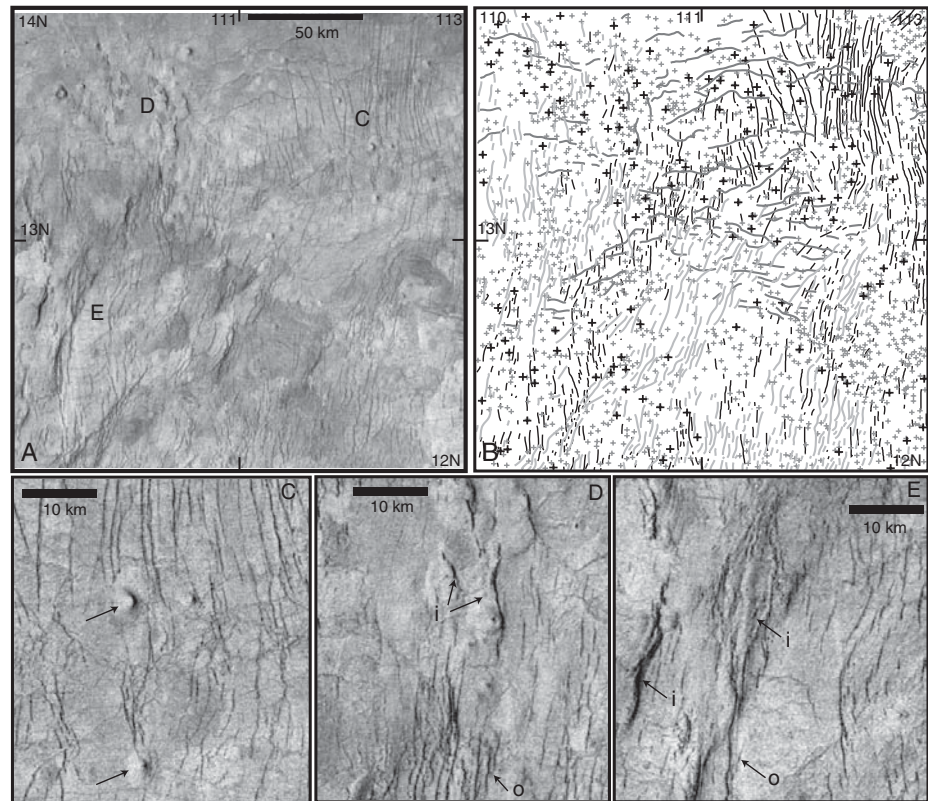
23N/103E (Fig. 4) hosts at least 402 definite shields and 754 combined shields, and NE-trending wrinkle ridges. Definite shields and potential shields have similar distributions, with slightly lower densities of definite shields in the northeast. An ~20-km-wide data gap obscures the central northern part of 23N/103E. Temporal relations between shields and wrinkle ridges are difficult to determine robustly, given the relatively small size and spacing of these primary and secondary structures, and given the fact that shields or variations in shield-paint thickness could contribute to strain partitioning during wrinkle-ridge formation. In some cases, it may appear as though a shield truncates a wrinkle ridge along trend and therefore would postdate wrinkle-ridge formation. However, it is also possible that the shield was emplaced prior to wrinkle-ridge formation, and ridge formation ended as it approached the shield. In addition, given the number of individual shields and individual wrinkle ridges, it is possible that wrinkle-ridge and shield formation overlapped in time. In the region between wrinkle ridges, a polygonal structure is best developed away from shield centers, indicating that the polygonal structures most likely formed after individual shields (also see Fig. 3C). The pattern likely reflects strain partitioning resulting from a thicker material layer near shield centers. But early polygonal fabric formation is also possible. The polygonal fabric shows either a preferred longitudinal shape parallel to the trend of the wrinkle ridges, or no preferred shape. In the southeast, shields are superposed on a locally preserved basal layer cut by closely spaced E-trending anastomosing lineaments (Fig. 4D). Locally NNW-striking fractures cut the shield paint, but the discontinuous nature of many fracture traces suggests that these fractures were locally reactivated; thus, original fractures likely predated most shield paint.

21N/113E (Fig. 5), which hosts at least 167 definite shields and 1080 combined shields,

area, chosen on the basis of data and geologic criteria, has both right- and left-illumination SAR images that lack large data gaps and that lack large impact craters or large tracts of ribbon terrain or fracture terrain, all of which could hamper shield identification and interrupt shield patterns. Map construction used four registered views: right- and left-illumination full-resolution SAR, each in normal and inverted mode.

I ranked shields by confidence levels: "definite shields" (obvious shields that most workers would be quite comfortable calling shields), and "potential shields" (possibly controversial features) (Table 1). The major distinction between these divisions relates to data resolution, and

as such to the experience of the mapper, as discussed above. Shields likely exist below SAR resolution, as noted above, thus making maximum estimates difficult to determine. Estimates of definite-shield densities across the five regions range from 3550 to 10,500 shields/10^6 km^2; these values represent minimum shield densities. Combined shield densities (both definite and potential shields) range from 15,650 to 33,675 shields/10^6 km^2; these values are neither minimum nor maximum values, but simply estimates.

There is no direct correlation between the number of definite shields and combined shields for individual regions. For example, 23N/103E hosts the fewest combined shields yet has the

shows similar relations with respect to wrinkle ridges and fractures. This region also preserves patches of extremely fine-scale polygonal fabric with diffuse to relatively sharp boundaries (Fig. 5C). Both definite and potential shields occur within the region of the fine polygonal fabric, the boundaries of which are not defined by obvious flow boundaries. Potential shields are more prominent in the region deformed by polygonal fabric; this might be a matter of contrast with a delicately textured substrate. Mottled areas free of small-scale polygonal fabric could be aggregates of subresolution shields. Wrinkle ridges cut the polygonal fabric boundary with no obvious spatial pattern relative to the fine polygonal fabric, indicating that there is likely a relative mechanical coherence in the layer across this boundary, although layer thickness may differ across the boundary. The region between wrinkle ridges preserves a fine-scale polygonal fabric; in fact, there appears to be a gradation in the scale of the polygonal structural fabric across the map area. NNW-striking fractures parallel to the regional trend are covered by shield paint, and yet locally, they cut individual shield edifices (Fig. 5C). An ~15-km-diameter circular depression marks the NE corner of 21N/113E; extremely fine, commonly covered fractures concentric to this structure extend 60–70 km from its center.

13N/111E (Fig. 6) displays 140 definite shields, 1340 combined shields, E-trending wrinkle ridges, and N-striking fractures. Locally, shields postdate formation of N-trending lineaments that both cut and invert shield-paint material (Fig. 6C). The lineaments are apparently extension fractures in places filled with shield-paint material, which were subsequently shortened and inverted, forming inversion structures (e.g., DeShon et al., 2000) (Figs. 6D, E). Fracture fill (shield paint), layer extension, and contraction were apparently extremely localized, as indicated by open fractures transitioning into inversion structures along strike and by close spatial location of open fractures and inversion structures. Detailed structural relations are perhaps most easily interpreted as evidence that both local extension and contraction postdate formation of many individual shields, but other individual shields postdate extension and contraction.

23N/117E (Fig. 7) hosts over 250 definite shields, 1000 combined shields, and inversion structures. In the northeast corner, patches of ribbon-terrain kipukas peek through a veil of shield terrain. Shield paint embays the detailed ribbon-terrain topography, comprising alternating parallel (N-trending) ridges and troughs (Hansen and Willis, 1998) (Fig. 7C). Shield paint blends into a coherent layer, with shields locally visible

Figure 6. Area 13N/111E; right-illuminated inverted SAR (A) and geologic map (B); symbols as in Figures 4 and 5; location of enlargements (C–E) shown in (A). Although many shields are cut by reactivated N-striking fractures, other shields clearly postdate fracture reactivation (C, arrows). Locally, shield-paint-filled fractures are inverted by later contraction, resulting in N-trending inversion structures. Folds or wrinkle ridges are marked by light gray lines in (B) and "i" in (D) and (E); open fractures are denoted with "o" (D and E); open fractures are locally modified along strike, either covered by shield deposits and/or forming inversion structures (E).
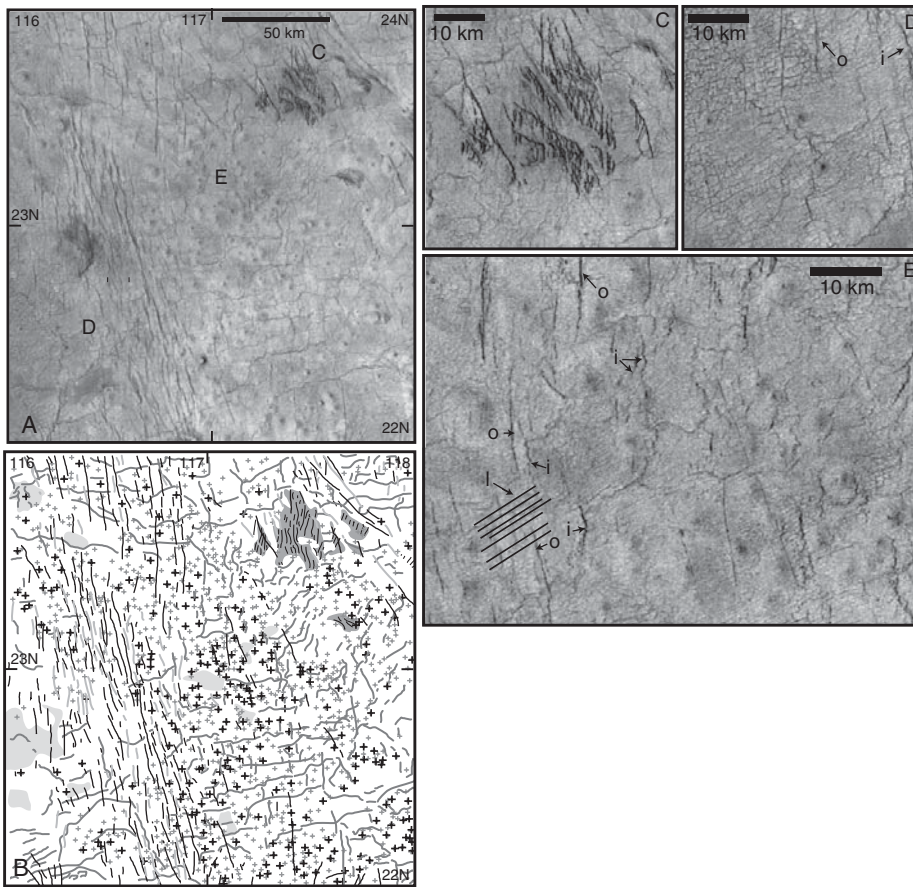
as a result of topographic expression. Isolated patches of fine-scale polygonal structures occur locally (Fig. 7D) and gradually increase in spacing away from the shields, consistent with an interpretation that shield paint is thicker near the edifices. Locally, a secondary structural fabric, marked by delicate, closely spaced (~500 m or less), short (~5–20 km) NE-trending lineaments (fractures?), transects the surface discontinuously (Fig. 7E). The fabric occurs in patches with a parallel lineament trend and similar lineament spacing from patch to patch. Fabric continuity across spatially separate regions supports the interpretation that this fabric is secondary. The tight lineament spacing likely reflects deformation of a thin layer, here interpreted as deformation of shield paint. Similar delicate lineament fabrics (with various orientations) occur across much of the Niobe-Greenaway map area.

13N/119E (Fig. 8) includes ribbon-terrain kipukas, E-trending wrinkle ridges, N-striking

fractures, and over 270 definite shields and 630 combined shields. Although not shown on the Niobe-Greenaway map (Fig. 2), regionally coherent ribbon trends exist across the region as preserved in isolated kipukas. In strong contrast to the fracture terrain illustrated in Figure 3B, the ribbon terrain in this region shows relatively high relief, rising from a ~6052-km radius to 6053 km along the northern edge. Shields and shield paint occur across the topographic range of ribbon terrain, forming high, isolated deposits (Fig. 8C). Even at high elevation, shield paint that flowed into localized lows gently masked ribbon fabrics (Fig. 8C), indicating that: (1) shield-terrain formation postdates ribbon-terrain formation here, (2) shield terrain forms discontinuously across local high relief (i.e., it cannot be connected by a continuous datum indicative of low-elevation embayment), and (3) shield paint is locally very thin. Regional continuity of ribbon trends between kipukas is consistent with the interpre-

Figure 7. Area 23N/117E; right-illuminated inverted SAR (A) and geologic map (B); symbols as in Figures 4–6; location of enlargements (C–E) shown in (A). Ribbon terrain (dark gray) shows ribbon trends (black lines); ribbon fabric is highlighted in (C); note that shield paint fills topographic lows of detailed ribbon terrain. Fine-scale polygonal fabric and open (reactivated?) fractures and inversion structures are apparent in (D) and (E). This region also shows a delicate, closely spaced, NE-trending lineament fabric ("l" in E).

tation that ribbon terrain extends beneath shield paint across much of the map area, and that shield terrain is thin at both a local and a regional scale. Delicate ENE-trending wrinkle ridges that cut shield paint east of the ribbon-terrain kipukas parallel regional trends (SE Fig. 8E). N-striking fractures both cut and are covered by shield paint, indicating that at least a part of the activity on these structures overlapped in time with shield-terrain formation.

POSSIBLE MODELS FOR SHIELD-TERRAIN FORMATION

Any model of shield-terrain formation must address the following observations. (1) Shields distributed across Niobe, Sogolon, and Llorona planitiae do not, qualitatively, define discernible patterns at any scale; (2) shields are not obviously aligned along major fractures (although higher-resolution data might reveal different relations), nor do they appear to cluster. (3) Shield terrain forms a thin, regionally extensive, but locally discontinuous, layer that variably veils early tectonic structures preserved in the preexisting crustal surface, and is variably cut as a result of local reactivation of these same structures. (4) Wrinkle ridges and polygonal fabrics generally deform shield paint. The delicate nature of wrinkle ridges, fractures, and inversion structures, as well as the regionally extensive distribution of these structures with little change in orientation, indicates that shield paint forms an extremely thin (locally absent) deposit that coalesces into a mechanical layer. (5) Shield terrain resides at a range of elevations, including as isolated occurrences in ribbon terrain (Fig. 9). (6) Shield terrain records local reactivation: shield paint covers early-formed fractures, which were apparently vari-

ably refractured, repainted (new shields), and experienced subsequent contraction resulting in structural inversion. (7) The regional scale shield-terrain substrate must have remained strong throughout shield-terrain formation and deformation. It is also likely that shield terrain is more globally extensive than currently recognized. Shield terrain occurs across V11 (Shimti Tessera; 25–50N/90–120E) and V12 (Vellamo Planitia; 25–50N/120–150E) (Aubele, 1996); V23 and V24 (0–25N/90–150E; see also Lang and Hansen, 2003), as discussed here; V4 (Atalanta Planitia; 50–75N/120–180E; Hansen, 2003); and southern V52 (Helen Planitia; 25–50S/240–270; López and Hansen, 2003). Three models of shield-terrain formation are considered below.

Flood-Lava Model

As noted above, lowland resurfacing is typically attributed to extensive catastrophically emplaced flood-type lava flows (e.g., Basilevsky and Head, 1996; Banerdt et al., 1997; Head and Coffin, 1997; Ivanov and Head, 2001b). This supposition forms the basis for two related hypotheses: catastrophic resurfacing (Strom et al., 1994) and global stratigraphy (e.g., Basilevsky and Head, 1996, 1998, 2002; Head and Basilevsky, 1998). These related hypotheses make specific predictions required by the crater density data within the context of catastrophic resurfacing: flood lava must be thick (1–3 km) and globally extensive (covering the lowlands), and it must have been emplaced very quickly, meaning <100 m.y., with ~10 m.y. most likely. The hypotheses further imply that "wrinkle-ridge plains" or "regional plains," the surface layer of Venus's vast lowlands (80% of the planet surface), including Niobe, Llorona, and Sogolon planitiae, represents this globally extensive 1–3-km-thick flood-lava unit. Thus, geologic relations from Niobe-Greenaway should provide a test of the catastrophic flood-lava hypothesis.
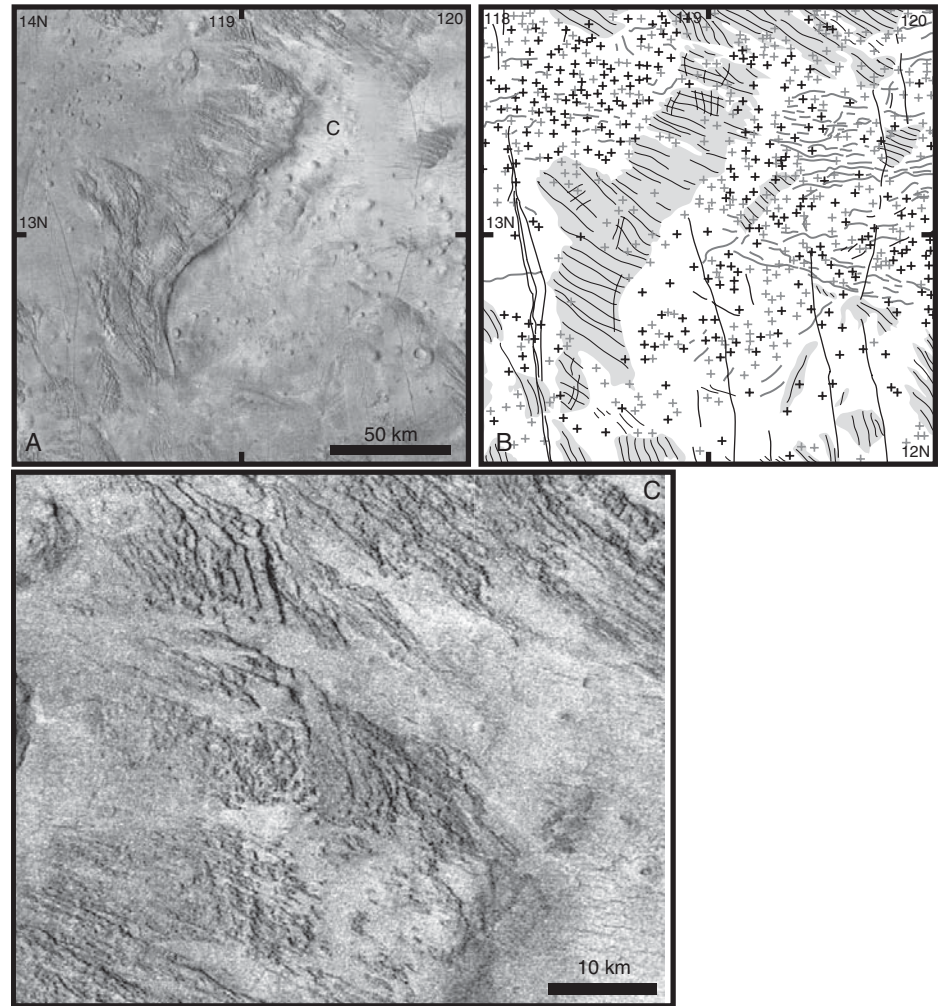
Collectively, the observations outlined above are difficult to accommodate within the catastrophic flood-lava hypothesis. The hypothesis calls for 1–3-km-thick flows, whereas shield terrain, which extends across 10,000,000 km², is tens of meters thick. The isolated kipukas of ribbon terrain and fracture terrain (basal, pre–flood-lava units in the catastrophic flood-lava hypothesis) are distributed across much of the map area, indicating very shallow depths to "basement." It is difficult to envision how a 1–3-km-thick layer could form lace-like shield terrain that variably and delicately veils and reveals its substrate. It is also difficult to envision how 1–3-km-thick lava flows could extend across topographically

V.L. HANSEN

complex terrain and occur in isolation at various elevations (e.g., Figs. 8 and 9).

Comparison of shield terrain with terrestrial flood lava provinces illustrates important differences in regional extent, lava thickness, and tectonic setting. Terrestrial flood lavas cover regions several orders of magnitude smaller than the area covered by shield terrain within the study area (Fig. 2) (Ernst and Buchan, 2001). Terrestrial flood lava typically erupts from relatively few sources and flows across the ground surface for extensive distances, but shield-terrain material emerged from individual eruptive centers across millions of square kilometers. Brief comparisons of shield terrain with the Snake River Plain and the Columbia River Basalt Province, both of the northwestern United States, are presented below.

The Snake River Plain, which covers ~36,000 km^2, displays shieldlike volcanic features that are similar to Venus shields in character (morphology), size (Greeley, 1982), and density (~5000 shields/10^6 km^2 [e.g., Kortz and Head, 2001]). Although the precise mode of formation of the Snake River Plain is debated, general geological facts are well known. The Snake River Plain forms a volcanotectonic province localized in a generally E-trending riftlike valley bounded by normal faults to the north and south. Geophysical data indicate that strike-slip faults dissect the interior, yet there is no evidence that "host" rocks from the north or south extend beneath lava flows within the Snake River Plain. That is, there is no evidence for pre-Cenozoic rocks, or basement material, within the Snake River Plain. The depth of volcanic material ranges up to 7–8 km with average thickness on the order of 1.5–2 km, although the actual value can be difficult to constrain.

Therefore, other than the surface expression of the volcanic plain, the Snake River Plain and shield terrain are vastly different. Shield terrain is not limited to a localized rift valley. Kipukas of isolated ribbon terrain and/or fracture terrain provide strong evidence of basement units across the study area. Eruptive centers in shield terrain are scattered across a region three orders of magnitude larger than the entire regional limit of Snake River Plains flows. The area illustrated in Figure 3B alone covers ~160,000 km^2, an order of magnitude larger area than the entire Snake River Plain; yet isolated eruptive centers are clearly delineated on the backdrop of the fracture-terrain basement. Each detailed map area of shield terrain (Figs. 4–8) covers ~40,000 km^2—areas individually larger than the entire Snake River Plain. Yet none of these areas shows any evidence to suggest the existence of tectonic boundaries. Clearly, the mode of volcanic emplacement is vastly different for Venus's

Figure 8. Area 13N/119E; right-illuminated inverted SAR (A) and geologic map (B); symbols as in Figures 4–7; location of enlargement (C) shown in (A). This region displays a large ribbon terrain inlier with several small inliers (medium gray). N-striking fractures are rare and relatively isolated. Shield paint fills local lows and gently masks older ribbon fabrics (C).

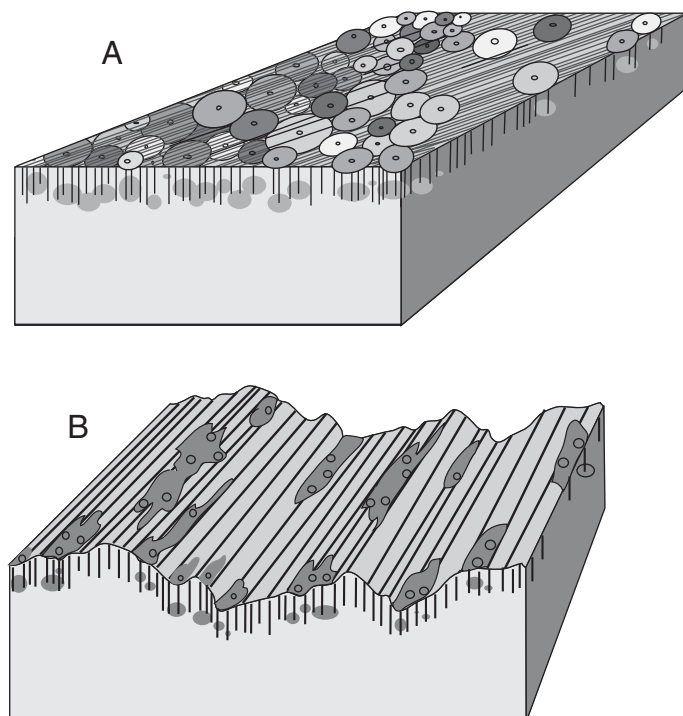extensively developed shield terrain than that of the spatially localized Snake River Plain.

The Columbia River Basalt Province, also in the northwestern United States and the youngest and perhaps best-studied classic terrestrial flood-lava province (e.g., Reidel and Hooper, 1989; Ernst and Buchan, 2001), might be better to compare with Venus's shield terrain. The Columbia River Basalt Province covers an area almost five times larger than the Snake River Plain (~164,000 km^2), although it is more than 50 times smaller than the extent of shield terrain within the study area (Fig. 2). The Columbia River Basalt Province lacks the distinctive morphological character of the Snake River Plain volcanic shields, and as such, morphological comparison with shield terrain is much less compelling. The Columbia River Basalt Province,

with a volume of ~170,000 km^3, ranges in thickness up to 5 km locally, with an average thickness of 1 km. The province includes ~300 individual flows with an average volume of 560 km^3 per flow. Linear vents occur in the eastern part of the province with individual vents as long as 150 km; such lengths would extend almost the

TABLE 1. NUMBERS AND DENSITIES OF DEFINITE-SHIELDS (DS) AND COMBINED SHIELDS (CS)

Center	DS	CS	DS/10^6 km^2	CS/10^6 km^2
23N/103E	402	626	10,500	15,650
21N/113E	167	1080	4175	27,000
13N/111E	142	1347	3550	33,675
23N/117E	251	1005	6275	25,125
13N/119E	271	631	7078	15,775

Figure 9. Cartoon block diagrams. (A) Highly schematic shields and shield paint and fracture relations; shield material emanates from local point sources at relatively shallow crustal levels (gray ellipses); material leaks upward along fractures, presumably driven by buoyancy forces and flows outward from individual centers. Local reactivation of fractures cut some shield deposits, but younger deposits cover fractures locally. (B) Shield terrain occurs as isolated exposures in topographically complex elevated ribbon terrain; source material apparently emerges from localized subsurface locations (gray shaded areas within the subsurface).

length of the detailed geologic maps (Figs. 4–8). Individual flows might reach 750 km.

Although the timing and mode of lava emplacement are debated, the relatively focused location of flow sources, the long vents, and the great length of individual flows are indications that the mode of emplacement of the Columbia River Basalt Province differs from that of Venus's shield terrain. Shield-terrain eruptive centers are distributed across over 10,000,000 km², a region that dwarfs the extent of the Snake River Plain and the Columbia River Basalt Province combined (Fig. 2). Eruptive centers responsible for all of the volcanic rocks of the Snake River Plain and the Columbia River Basalt Province must be confined to a relatively small area indicated by the dashed line box in Figure 2. Additionally, individual shield-terrain flows are extremely small in comparison to individual flows within the Columbia River Basalt Province. Clearly the mode of volcanic emplacement, and presumably lava formation, must be different for the Venus province as compared to these terrestrial provinces. The volume of Columbia River Plateau basalt spread

evenly over the ~10,000,000 km² of study area covered by shield terrain would be ~17 m thick. This value is two orders of magnitude thinner than the 1–3 km called for in the catastrophic flood-lava hypothesis.

Another significant problem with the catastrophic flood-lava hypothesis involves magma storage. In addition to requiring a huge volume of magma (10,000,000–30,000,000 km³) just to cover the lowlands in the study area, the magma required for catastrophic flooding of this region would have had to be stored at depth. Given that eruptive centers pepper the ~10,000,000 km² region of shield terrain, the magma should be stored locally across the entire region. However, it would seem that the existence of such a large subsurface magma body would impose differential stresses across the overlying surface; and such differential stresses, if they had existed, should be reflected in surface strain features such as wrinkle ridges or fractures. Yet across the study area, wrinkle ridges and fractures parallel broad regional trends that are consistent with loading by Aphrodite Terra (Sandwell et al., 1997), and do not seem to reflect the size, shape,

or presence of a large subsurface magma body. Even if one considered two (or more) separate magma bodies (one each under Niobe, Sogolon, and Llorona planitiae), each subsurface magma body would have a minimum sill-like diameter of ~1500 km (likely larger, as Niobe and Llorona each extend >1000 km north of the map area). It seems difficult to "hide" such large subsurface magma bodies. In addition, the crust or surface upon which shield terrain is emplaced displays apparent strength throughout shield terrain development, contrary to what would be expected above a regionally extensive subsurface magma body. We might expect large radial fracture patterns reflecting dikes and subsurface magma transport, as observed in large terrestrial igneous provinces (e.g., Ernst and Buchan, 2001), but there is no evidence of these regional tectonic patterns within the study area (Fig. 2). It is also difficult to justify how large subsurface magma chambers could preserve shallow, yet extensive, crustal patterns of preexisting surfaces such as ribbon or fracture terrain. Additionally, a large subsurface magma body would more likely result in large focused eruptions to the surface rather than numerous, closely spaced (on the order of kilometers), small eruptions. If the magma source was deep and emerged to the surface, then the thousands of individual eruptive centers are difficult to justify.

Perhaps thousands of individual eruptive centers could exist above a huge subsurface magma body if the crust were porous to magma, and magma could leak to the surface like thousands of groundwater-like seeps. However, such a scenario is inconsistent with the preservations of numerous isolated kipukas of basal ribbon terrain and fracture terrain, among other considerations.

A model of numerous small subsurface magma chambers (so as not to disturb the surface and leave evidence of their subsurface existence) through time to accommodate the close shield spacing would not address the very fast emplacement of flood lava as required by the flood-lava catastrophic resurfacing model, and the problems alluded to here with regard to lava flow thickness would remain. Thus, the regional extent of shield terrain and the incredible number and extensive distribution of eruptive centers seem paradoxical and hard to accommodate within the global and catastrophic flood-lava hypothesis.

Mud Volcano Model

The catastrophic flood-lava hypothesis for lowland resurfacing does not address, among other things, the occurrence of thousands of small individual eruptive centers across a vast low-relief region with little evidence of focused

tectonic activity. In order to address this particular concern, it could be useful to turn to terrestrial ocean basins, which might provide the closest analog for a similar regional setting on Earth. We must be mindful, however, that the mere presence of Earth's kilometer deep oceans inhibit extensive analysis of the ocean-basin surface at a scale and resolution required to make comparisons with Venus's lowland. Despite this limitation, recent studies of parts of Earth's ocean floor reveals data useful to consider here—the occurrence of submarine mud volcanoes whose morphology, size, and spacing (e.g., Graue, 2000; Dimitrov, 2002) are similar to shields of Venus's shield terrain.

Shield morphology aside, why would terrestrial mud volcanoes, which require vast quantities of liquid water, merit comparison with Venus's shield terrain? Clearly, Venus's ultradry surface currently harbors no liquid water (e.g., Donahue and Russell, 1997; Donahue et al., 1997). However, the present is not always the key to the past. Earth's current environmental conditions are vastly different from ancient terrestrial conditions, and Venus's past environmental conditions were likely different as well.

As noted in the section on Venus's surface environment, Venus could have hosted an ancient global ocean. The high deuterium/hydrogen ratio of Venus's atmosphere is consistent with the interpretation that Venus once held the equivalent of a global ocean with a depth of 4–530 m (Donahue et al., 1982; Donahue and Russell, 1997; Hunten, 2002). The presence of a Venusian global ocean has also been proposed on the basis of geological interpretation of Venus channels; Jones and Pickering (2003) argued that channels across Venus formed as subaqueous channels similar to terrestrial submarine channels. Whether Venus's channels formed in this manner, or whether they represent other processes entirely (e.g., Baker et al., 1997), is outside the scope of this contribution. However, given the morphological similarity of submarine terrestrial mud volcanoes to Venus's shield-terrain shields, a mud volcano hypothesis for shield-terrain formation is pursued further herein.

The widespread development of numerous shallow eruptive sources could result from water (or fluid)-saturated sediments with eruptions of mud, forming volcanoes. Mud volcanoes have been recognized in increasingly larger numbers and across broader regional areas with ocean-floor exploration at an effective resolution consistent with mud volcano identification (e.g., Graue, 2000; Dimitrov, 2002). Mud volcanoes range in size from tens of meters to 3–4 km in diameter with heights to ~500 m; they display a wide range of morphologies, including plateau shapes that are peaked, flat, mounded, or fun-

nel-shaped. Mud volcanoes occur in a range of tectonic environments, from convergent margin setting (including on accretionary complexes), to deltaic regimes, to passive margin settings, and they are commonly spatially (and likely temporally) associated with both extensional and contractional tectonic structures.

Submarine mud volcanoes in particular, such as those described from deepwater Nigeria (Graue, 2000), might provide analogs for Venus's shield paint. The 1–2-km-diameter Nigerian mud volcanoes show spatial association with numerous pockmarks (which may be similar to Venusian features mapped as small shields herein) and cuspate faults. Mud volcanoes can erupt fine-grained mud matrix or mud breccia with millimeter- to meter-sized clasts. Thus, in SAR images, flow material could be either radar-dark or -bright. Although much is unknown about terrestrial mud volcanoes, they are generally associated with rapid deposition of thick young (Tertiary or younger) sediments, with sediment piles several kilometers thick, up to perhaps 10–12 km. Rapid sedimentation of dominantly clay-to-silt sediments apparently causes under-compaction and overpressuring of buried deposits, setting the stage for subsequent focused mud eruptions. Mud volcanoes might require fine-grained overburden gas-charged deposits over 1.5–2 km deep in a sedimentary section, continuous hydrocarbon (or other gas) generation, and active tectonism (Dimitrov, 2002).

By analogy, shield paint might represent coalesced eruptions of numerous mud volcanoes. At first glance, it might seem that the apparent strength of the shield paint with its ability to host fracture and fold suites, and that the time-transgressive character of shield-terrain formation and deformation are inconsistent with a mud volcano hypothesis. However, broad, synchronous development of mud volcanoes and local deformation occur on Earth (e.g., Graue, 2000). Mud volcanoes, together with wrinkle ridges, polygonal fabrics, reactivated extension fractures, and inversion structures, could have formed in an ancient Venus ocean floor environment or as a result of ancient ocean desiccation.

More significant problems with a mud volcano origin of shield terrain might be the apparent discontinuous or lacelike nature of shield paint, and the thin layer thickness of shield material above the ribbon terrain or fracture terrain basement. If the Venusian lowlands once held ancient oceans one might expect sedimentary cover to be pervasive, draping (and presumably completely burying) ribbon-terrain topography more equitably than observed. In addition, a requirement of several kilometers of sediment for mud volcano formation is at odds with the occurrence of small isolated shield ter-

rain outcrops entirely surrounded by older basal ribbon terrain or fracture terrain (e.g., Fig. 3B) and with the regionally thin character of shield terrain. Perhaps ocean currents influenced deposition and thus somehow contributed to uneven sediment draping, but this explanation could not account for thin isolated shield terrain (mud volcanoes and host sediment). Presumably, mud volcanoes would be difficult to form in isolation on ribbon terrain or fracture terrain (e.g., Fig. 3B), given that there would not be an obvious source of sediment on basal terrain to form the mud volcanoes. Additionally, isolated shield terrain is clearly not several kilometers thick, as seems to be required for the mud volcano hypothesis. Although sediment could have been removed after mud volcano eruption to exposed ribbon or fracture terrain substrate, there is no obvious evidence of widespread erosion (or subsequent deposition) or shield truncation to support this scenario. Thus, although a mud volcano model might address extensive development of numerous closely spaced point-source eruptions, such a model does not appear consistent with documented detailed geologic relations.

In Situ Partial Melt Model

A third class of model to consider is shield-terrain formation resulting from in situ point-source partial melting of the crust (tertiary melt formation) with subsequent rise of melt to the surface along, presumably preexisting, fracture conduits. It would seem most likely that shield forming melt was of relatively low viscosity in order to migrate to the surface, although the range of individual shield morphologies may imply a range of melt viscosity, or melt crystallinity. Melt could rise because of buoyancy, driven by density contrast between the melt and the surrounding material. Such a contrast could result from differences in composition, temperature, or a combination.

But what could cause shallow, point-source partial melt in the crust over extensive regions? Incipient point source partial melting of the crust might result from a regional elevated thermal profile. Hansen and Bleamaster (2002) proposed that incipient point source partial melting could be induced or enhanced if the temperature of a rock mass, together with local radioactive element concentration, pushes the host rock into a partial melt condition. Partial melting of basalt can also occur because of the addition of water at depth (e.g., Green, 1982; Thompson, 2001). Water can be carried to depth through subduction processes, as on Earth; or water could exist in hydrated minerals and be released at depth as a result of dehydration reactions (e.g., Beard and Lofgren, 1991).

Is it possible that Venus's crust could have experienced in situ partial melting as a result of dehydration reactions? Such a hypothesis requires a hydrated Venus crust, which in turn requires water. As noted above, current data are consistent with the notion that Venus could have had an ancient global ocean, and as such, Venus's basaltic crust could have become hydrated—presumably altered to amphibole mineralogy (e.g., Johnson and Fegley, 2000, 2003).

Even if Venus's surface did not host widespread oceans, water could have existed in a more localized way in time or space through delivery by icy comets. Icy comets could deliver water to Venus at a rate equal to or greater than exospheric escape over the last billion years (Bullock and Grinspoon, 2001). Because comet size and flux were greater in the past, the amount of water that could have been delivered to Venus by icy comets could have been even greater prior to 1 billion years ago. For example, a billion-year-ago comet could deliver as much as 40 times the current atmospheric abundance of H_2O in an instant (Bullock and Grinspoon, 2001). Icy comet water could have contributed to basalt hydration in localized regions or across the planet. Thus, Venus's basaltic crust could have been hydrated in an ancient ocean setting, as icy comets delivered water to an ancient Venus, or both. The idea of widespread hydration of Venus's crust is not new. Lecuyer et al. (2000) argued that Venus once had a volume of water similar to that of Earth, and that a combination of crustal hydration and hydrogen escape processes could explain the present-day low amount and high deuterium/hydrogen ratio of water in the Venusian atmosphere. Thus, widespread hydration of an ancient basaltic crust on Venus seems feasible given the available data.

Assuming a hydrated basaltic Venusian crust, Venus's current environmental conditions (e.g., ~750 K, dry, 92 bars CO_2) would not result in formation of shallow partial melt. However, Venus was not only likely wetter in the past, but also hotter because of higher levels of greenhouse gases (Bullock and Grinspoon, 1996, 2001). Climate models indicate that ancient surface temperature could have reached or exceeded 1000 K (Phillips et al., 2001), resulting in a relatively steep thermal gradient. An elevated thermal gradient could trigger dehydration of previously hydrated basaltic crustal material at shallow crustal levels; dehydration could in turn cause shallow in situ partial melting of hydrous basalt (Green, 1982) or, perhaps more likely, continued amphibole dehydration and resulting partial melting (e.g., Beard and Lofgren, 1991; Zolotov et al., 1997; Johnson and Fegley, 2000, 2003; Thompson, 2001).

Partial melt (presumably tertiary), once formed, could rise to the surface along fractures.

Strong infrared absorption by the high-density CO_2 atmosphere would insulate melt, enhance low viscosity, and lead to extremely slow cooling as a result of the inability of the melt to release heat due to low convective heat loss at high atmospheric pressure (e.g., Snyder, 2002). A low melt-surface temperature differential would further slow crystallization (Stofan et al., 2000). Thus, elevated concentrations of radioactive elements, global high temperature, or a combination could trigger shallow in situ partial melting and allow melt that emerged from numerous individual centers to coalesce into a extensive, discontinuous, yet coherent, thin shield paint at the surface. Crystallized shield paint could form a thin mechanically coherent layer that could be deformed by fractures, folds, warps, wrinkle ridges, and inversion structures, whereas regional crust (substrate) would remain strong. The in situ partial melt process might be compared to partial melting in terrestrial migmatite terrain, with partial melt escaping to local low-pressure regions, resulting in local differentiation. Similarly, the in situ partial melt hypothesis proposed here could result in local crustal differentiation, with shield terrain forming a thin layer of more felsic material (e.g., Fig. 9). This process could occur independent of surface elevation, with individual packets of partial melt leaked to the surface from thousands of subsurface locations where in situ partial melting occurred. The thousands of individual eruptive centers could leak material to the surface where it could coalesce, forming shield paint.

Detailed discussion of partial melt formation by concentration of radioactive elements or dehydration reactions is nontrivial and beyond the scope of the current contribution. Either mechanism could favor specific terrain that was predisposed to such reactions. Research that delves into in situ partial melting should consider that carbon dioxide or water could have existed as supercritical fluids.

High global temperatures predicted by climate models (e.g., Bullock and Grinspoon, 1996, 2001; Phillips et al., 2001) could spur shield-terrain formation via in situ partial melting of previously hydrated basaltic crust. Local heating and cooling could provide thermal stresses leading to contraction and extension of the shield-terrain layer, resulting in wrinkle-ridge formation (e.g., Anderson and Smrekar, 1999; Solomon et al., 1999) and fracture-fill inversion of the thin, regionally extensive, shield-paint layer.

SUMMARY AND IMPLICATIONS

The data presented here do not support the catastrophic flood-lava hypothesis for Venus's resurfacing. The catastrophic flood-lava hypothesis calls for the emplacement of 1–3-km-thick flood-lava across Venus's lowland regions. But the lowland within the study area is covered by a thin, locally discontinuous layer of shield terrain marked by thousands of small eruptive centers distributed across the entire region. The shield-terrain layer lies directly above basal ribbon terrain or fracture terrain and cannot accommodate the 1–3-km thickness of flood lava required by the catastrophic flood-lava hypothesis. The occurrence of shield terrain therefore requires renewed consideration of Venus resurfacing processes that operated across the lowland.

The mud volcano and in situ partial melt models for shield-terrain formation have vastly different implications for Venus's evolution, and yet both models might suggest a wet ancient Venus. The mud volcano hypothesis would seem to require the occurrence of a moderately deep, globally extensive ocean. The water required by the in situ partial melt hypothesis would not have had to exist as a thick globally extensive layer but would require basalt hydration. Both hypotheses can be accommodated within, but do not require, a global evolutionary framework that includes an ancient thin lithosphere and a contemporary thick lithosphere, a view supported by many data sets, numerical models, and theoretical arguments (e.g., Grimm, 1994; Solomatov and Moresi, 1996; Schubert et al., 1997; Hansen and Willis, 1998; Phillips and Hansen, 1998). If the spirit of either model is correct, the presence of global water would likely change crustal rheology, which could, in turn, affect the formation and evolution of crustal plateaus and ancient impact craters. In addition, impact craters formed on thin global lithosphere or in the presence of a global ocean might have quite a different signature than Venus's ~970 "pristine" impact craters. Thus, Venus's surface could record a significantly longer history than ca. 750 Ma, an average model surface age based solely on currently recognized (pristine) impact craters. High global temperatures predicted by climate models (e.g., Bullock and Grinspoon, 1996, 2001; Phillips et al., 2001) could spur shield-terrain formation via in situ partial melting; or high global temperature could result in boiling and evaporation of a global ocean, leaving behind mud volcanoes and desiccation structures including wrinkle ridges, polygonal fabrics, and inversion structures. The presence of global water would also affect climate itself and thus have implications for current climate models, as pointed out by Bullock and Grinspoon (2001).

The catastrophic flood-lava hypothesis falls short in accommodating the location, density, and character of extensive shield terrain. The mud volcano hypothesis also has problems as discussed; however, given that this hypothesis

predicts such different evolutionary conditions and history for Venus, it perhaps should be explored further. Although existing data favor the in situ partial melt model because it seems to best explain geological relations, given the large number of unknowns with regard to Venus's evolution, it would seem scientifically capricious to discount either the mud volcano or partial melt model at this point (e.g., Gilbert, 1886; Chamberlin, 1897). Perhaps someone will present arguments that favor the flood-lava hypothesis in addressing the observations presented herein; however, I cannot currently see a way to continue to entertain this hypothesis in light of the data presented here.

Both the mud volcano and partial melt hypotheses can be tested with global detailed mapping, and petrologic modeling and experiments. In the case of a partial melt origin, all the material in shield terrain would emerge from below the surface, whereas in the case of a mud volcano origin, shield terrain would represent sedimentary material deposited from above, either as local gravity-driven fluid flows or as suspension-deposited sediment that settled out of a water column (or other fluid column). Shields that lack an edifice could be small mud diapirs, or they could be small bubbles of partial melt that did not release volatiles, resulting in a sort of explosion pit. The mud volcano hypothesis predicts that the vast lowland surface (shield paint) is sedimentary in origin, whereas the partial melt hypothesis predicts that the shield paint comprises a thin veneer of crystallized tertiary melt.

Of course, it is also possible that not all shields are formed in the same manner; shield terrain may form by more than one method, which may differ substantially from the formation of shield clusters (not addressed herein). Both the mud volcano and partial melt hypotheses suggest that Venus was wet in the past and hence might have harbored or nursed water-based life as we know it. Whatever the mechanism or means of the formation of shield terrain, its existence is difficult to reconcile with thick (1–3 km), catastrophically emplaced globally extensive flood-lava flows. Thus, the existence of shield terrain seems to provide significant challenges to the related catastrophic resurfacing and global stratigraphy views of Venus's evolution.

ACKNOWLEDGMENTS

REFERENCES CITED

Anderson, F.S., and Smrekar, S.E., 1999, Tectonic effects of climate change on Venus: Journal of Geophysical Research, v. 104, p. 30,743–30,756, doi: 10.1029/1999JE001082.

Aubele, J., 1996, Akkruva small shield plains; definition of a significant regional plains unit on Venus: Lunar and Planetary Science, v. 27, p. 49–50.

Aubele, J.C., and Slyuta, E.N., 1990, Small domes on Venus: Characteristics and origin: Earth, Moon, and Planets, v. 50/51, p. 493–532, doi: 10.1007/BF00142404.

Baker, V.R., Komatsu, G., Gulick, V.C., and Parker, T.J., 1997, Channels and valleys, in Bouger, S.W., Hunten, D.M., and Phillips, R.J., eds., Venus II—Geology, geophysics, atmosphere, and solar wind environment: Tucson, University of Arizona Press, p. 757–798.

Banerdt, W.B., McGill, G.E., and Zuber, M.T., 1997, Plains tectonics on Venus, in Bouger, S.W., Hunten, D.M., and Phillips, R.J., eds., Venus II—Geology, geophysics, atmosphere, and solar wind environment: Tucson, University of Arizona Press, p. 901–930.

Basilevsky, A.T., and Head, J.W., 1996, Evidence for rapid and widespread emplacement of volcanic plains on Venus: Stratigraphic studies in the Baltis Vallis region: Geophysical Research Letters, v. 23, p. 1497–1500, doi: 10.1029/96GL00975.

Basilevsky, A.T., and Head, J.W., 1998, The geologic history of Venus: A stratigraphic view: Journal of Geophysical Research, v. 103, p. 8531–8544, doi: 10.1029/98JE00487.

Basilevsky, A.T., and Head, J.W., 2002, Venus: Timing and rates of geological activity: Geology, v. 30, p. 1015–1018, doi: 10.1130/0091-7613(2002)0302.0.CO;2.

Basilevsky, A.T., Head, J.W., Schaber, G.G., and Strom, R.G., 1997, The resurfacing history of Venus, in Bouger, S.W., Hunten, D.M., and Phillips, R.J., eds., Venus II—Geology, geophysics, atmosphere, and solar wind environment: Tucson, University of Arizona Press, p. 1047–1086.

Beard, J.S., and Lofgren, G.E., 1991, Dehydration melting and water-saturated melting of basaltic and andesitic greenstones and amphibolites at 1, 3, and 6.9 kb: Journal of Petrology, v. 32, p. 365–401.

Bridges, N.T., 1995, Submarine analogs to Venusian pancake domes: Geophysical Research Letters, v. 22, p. 2781–2784, doi: 10.1029/95GL02662.

Bridges, N.T., 1997, Ambient effects on basalt and rhyolite lavas under Venusian, subaerial, and subaqueous conditions: Journal of Geophysical Research, v. 102, p. 9243–9257, doi: 10.1029/97JE00390.

Bullock, M.A., and Grinspoon, D.H., 1996, The stability of climate on Venus: Journal of Geophysical Research, v. 101, p. 7521–7530, doi: 10.1029/95JE03862.

Bullock, M.A., and Grinspoon, G.H., 2001, The recent evolution of climate on Venus: Icarus, v. 150, p. 19–37, doi: 10.1006/icar.2000.6570.

Campbell, B.A., 1999, Surface formation rates and impact crater densities on Venus: Journal of Geophysical Research, v. 104, p. 21,951–21,955, doi: 10.1029/1998JE000607.

Campbell, B.A., and Rogers, P.G., 2002, Geologic map of the Bell Regio (V9) quadrangle, Venus: U.S. Geological Survey Geologic Investigations Series Map I-2743, scale 1:5,000,000.

Chapman, M.G., 1999, Geologic map of the Galindo (V40) quadrangle, Venus: U.S. Geological Survey Geologic Investigations Series Map I-2613, scale 1:5,000,000.

Chapman, M.G., and Zimbelman, J.R., 1998, Corona associations and their implications for Venus: Icarus, v. 132, p. 344–361, doi: 10.1006/icar.1998.5899.

Crumpler, L.S., Aubele, J.C., Senske, D.A., Keddie, S.T., Magee, K.P., and Head, J.W., 1997, Volcanoes and centers of volcanism on Venus, in Bouger, S.W.,

Chamberlin, T.C., 1897, The method of multiple working hypotheses: Journal of Geology, v. 5, p. 837–848.

Hunten, D.M., and Phillips, R.J., eds., Venus II—Geology, geophysics, atmosphere, and solar wind environment: Tucson, University of Arizona Press, p. 697–756.

DeShon, H.R., Young, D.A., and Hansen, V.L., 2000, Geologic evolution of southern Rusalka Planitia, Venus: Journal of Geophysical Research, v. 105, p. 6983–6995, doi: 10.1029/1999JE001155.

Dimitrov, L.I., 2002, Mud volcanoes—The most important pathway for degassing deeply buried sediments: Earth-Science Reviews, v. 59, p. 49–76, doi: 10.1016/S0012-8252(02)00069-7.

Donahue, T.M., 1999, New analysis of hydrogen and deuterium escape from Venus: Icarus, v. 141, p. 226–245, doi: 10.1006/icar.1999.6186.

Donahue, T.M., and Russell, C.T., 1997, The Venus atmosphere and ionosphere and their interaction with the solar wind: An overview, in Bouger, S.W., Hunten, D.M., and Phillips, R.J., eds., Venus II—Geology, geophysics, atmosphere, and solar wind environment: Tucson, University of Arizona Press, p. 3–31.

Donahue, T.M., Grinspoon, D.H., Hartle, R.E., and Hodges, R.R., 1997, Ion/neutral escape of hydrogen and deuterium: Evolution of water, in Bouger, S.W., Hunten, D.M., and Phillips, R.J., eds., Venus II—Geology, geophysics, atmosphere, and solar wind environment: Tucson, University of Arizona Press, p. 385–414.

Donahue, T.M., Hoffman, J.H., Hodges, R.R., and Watson, A.J., 1982, Venus was wet: A measurement of the ratio of deuterium to hydrogen: Science, v. 216, p. 630–633.

Ernst, R.E., and Buchan, K.L., 2001, Large mafic magmatic events through time and links to mantle plume-heads, in Ernst R.E., and Buchan, K.L., eds., Mantle plumes: Their identification through time: Geological Society of America Special Paper 352, p. 483–509.

Ford, P.G., and Pettengill, G.H., 1992, Venus topography and kilometer-scale slopes: Journal of Geophysical Research, v. 97, p. 13,103–13,114.

Ford, J.P., Plaut, J.J., Weitz, C.M., Farr, T.G., Senske, D.A., Stofan, E.R., Michaels, G., and Parker, T.J., 1993, Guide to Magellan image interpretation: National Aeronautics and Space Administration Jet Propulsion Laboratory Publication 93-24, 287 p.

Ghent, R.R., and Tibuleac, I.M., 2002, Ribbon spacing in Venusian tessera: Implications for layer thickness and thermal state: Geophysical Research Letters, v. 29, no. 20, doi:10.1029/2002GL015994.

Gilbert, G.K., 1886, Inculcation of the scientific method: American Journal of Science, v. 31, p. 284–299.

Gilmore, M.S., Collins, G.C., Ivanov, M.A., Marinangeli, L., and Head, J.W., 1998, Style and sequence of extensional structures in tessera terrain, Venus: Journal of Geophysical Research, v. 103, p. 16,813–16,840, doi: 10.1029/98JE01322.

Graue, K., 2000, Mud volcanoes in deepwater Nigeria: Marine Petroleum Geology, v. 17, p. 959–974, doi: 10.1016/S0264-8172(00)00016-7.

Greeley, R., 1982, The Snake River Plain, Idaho: Representative of a new category of volcanism: Journal of Geophysical Research, v. 87, p. 2705–2712.

Green, T.H., 1982, Anatexis of mafic crust and high-pressure crystallization of andesite, in Thorpe, R.S., ed., Andesites: London, Wiley, p. 465–487.

Grimm, R.E., 1994, Recent deformation rates on Venus: Journal of Geophysical Research, v. 99, p. 23,163–23,171, doi: 10.1029/94JE02196.

Grimm, R.E., and Hess, P.C., 1997, The crust of Venus, in Bouger, S.W., Hunten, D.M., and Phillips, R.J., eds., Venus II—Geology, geophysics, atmosphere, and solar wind environment: Tucson, University of Arizona Press, p. 1205–1244.

Guest, J.E., Bulmer, M.H., Aubele, J.C., Beratan, K., Greeley, R., Head, J.W., Michaels, G., Weitz, C., and Wiles, C., 1992, Small volcanic edifices and volcanism in the plains on Venus: Journal of Geophysical Research, v. 97, p. 15,949–15,966.

Hansen, V.L., 2000, Geologic mapping tectonic planets: Earth and Planetary Science Letters, v. 176, p. 527–542, doi: 10.1016/S0012-821X(00)00017-0.

Hansen, V.L., 2002, Preliminary geologic mapping of Niobe Planitia quadrangle (V-23), Venus [abs.], in Gregg, T.K.P., Tanaka, K., and Senske, D., eds., Abstracts of the Annual Planetary Geologic Mappers Meeting, 2002: U.S. Geological Survey Open-File Report 02-412, p. 35–37.

Hansen, V.L., 2003, In situ partial melt on Venus: Evidence for ancient water?: Lunar and Planetary Science, v. 34, p. 1152.

Hansen, V.L., and Bleamaster, L.F., 2002, Distributed point source volcanism: A mechanism for "regional plains" resurfacing Venus: Lunar and Planetary Science, v. 33, p. 1061.

Hansen, V.L., and DeShon, H.R., 2002, Geologic map of Diana Chasma quadrangle (V37), Venus: U.S. Geological Survey Geologic Investigations Series Map I-2752, scale 1:5,000,000.

Hansen, V.L., and Willis, J.J., 1998, Ribbon terrain formation, southwestern Fortuna Tessera, Venus: Implications for lithosphere evolution: Icarus, v. 132, p. 321–343, doi: 10.1006/icar.1998.5897.

Hansen, V.L., Banks, B.K., and Ghent, R.R., 1999, Tessera terrain and crustal plateaus, Venus: Geology, v. 27, p. 1071–1074, doi: 10.1130/0091-7613(1999)0272.3.CO;2.

Hansen, V.L., Willis, J.J., and Banerdt, W.B., 1997, Tectonic overview and synthesis, in Bouger, S.W., Hunten, D.M., and Phillips, R.J., eds., Venus II—Geology, geophysics, atmosphere, and solar wind environment: Tucson, University of Arizona Press, p. 797–844.

Hansen, V.L., Phillips, R.J., Willis, J.J., and Ghent, R.R., 2000, Structures in tessera terrain, Venus: Issues and answers: Journal of Geophysical Research, v. 105, p. 4135–4152, doi: 10.1029/1999JE001137.

Hauck, S.A., Phillips, R.J., and Price, M.H., 1998, Venus: Crater distribution and plains resurfacing models: Journal of Geophysical Research, v. 103, p. 13,635–13,642, doi: 10.1029/98JE00400.

Head, J.W., and Basilevsky, A.T., 1998, Sequence of tectonic deformation in the history of Venus: Evidence from global stratigraphic relations: Geology, v. 26, p. 35–38, doi: 10.1130/0091-7613(1998)0262.3.CO;2.

Head, J.W., and Coffin, M.F., 1997, Large igneous provinces: A planetary perspective, in Mahoney, J.J., and Coffin, M.F., eds., Large igneous provinces: Continental, oceanic, and planetary flood volcanism: Geophysical Monograph Series: Washington, D.C., American Geophysical Union, p. 411–438.

Head, J.W., Crumpler, L.S., Aubele, J.C., Guest, J.E., and Saunders, R.S., 1992, Venus volcanism: Classification of volcanic features and structures, associations, and global distribution from Magellan data: Journal of Geophysical Research, v. 97, p. 13,153–13,198.

Herrick, R.R., and Sharpton, V.L., 2000, Implications from stereo-derived topography of Venusian impact craters: Journal of Geophysical Research, v. 105, p. 20,245–20,262, doi: 10.1029/1999JE001225.

Herrick, R.R., Sharpton, V.L., Malin, M.C., Lyons, S.N., and Feely, K., 1997, Morphology and morphometry of impact craters, in Bouger, S.W., Hunten, D.M., and Phillips, R.J., eds., Venus II—Geology, geophysics, atmosphere, and solar wind environment: Tucson, University of Arizona Press, p. 1015–1046.

Hunten, D.M., 2002, Exospheres and planetary escape, in Mendillo, M., Nagy, A., and Waite, J.H., eds., Atmospheres in the solar system: Comparative aeronomy: American Geophysical Union Geophysical Monograph 130, p. 191–202.

Ivanov, M.A., and Head, J.W., 1996, Tessera terrain on Venus; a survey of the global distribution, characteristics, and relation to surrounding units from Magellan data: Journal of Geophysical Research, v. 101, p. 14,861–14,908, doi: 10.1029/96JE01245.

Ivanov, M.A., and Head, J.W., 2001a, Geologic map of the Lavinia Planitia quadrangle (V-55), Venus: U.S. Geological Survey Geologic Investigations Series Map I-2684, scale 1:5,000,000.

Ivanov, M.A., and Head, J.W., 2001b, Geology of Venus: Mapping of a global geotraverse at 30°N latitude: Journal of Geophysical Research, v. 106, p. 17,515–17,566, doi: 10.1029/2000JE001265.

Johnson, N.M., and Fegley, B.J., Jr., 2000, Water on Venus: New insights from tremolite decomposition: Icarus, v. 146, p. 301–306, doi: 10.1006/icar.2000.6392.

Johnson, N.M., and Fegley, B.J., Jr., 2003, Tremolite decomposition on Venus II: Products, kinetics, and mechanism: Icarus, v. 164, p. 317–333, doi: 10.1016/S0019-1035(03)00102-7.

Johnson, J., Komatsu, G., and Baker, V., 1999, Geologic map of Barrymore quadrangle (V59), Venus: U.S. Geological Survey Geologic Investigations Series Map I-2610, scale 1:5,000,000.

Jones, A.P., and Pickering, K.T., 2003, Evidence for aqueous fluid-sediment transport and erosional processes on Venus: Journal of Geological Society London, v. 160, p. 319–327.

Kirk, R., Soderblom, L., and Lee, E., 1992, Enhanced visualization for interpretation of Magellan radar data: Supplement to the Magellan special issue: Journal of Geophysical Research, v. 97, p. 16,371–16,380.

Kortz, B.E., and Head, J.W., 2001, Comparisons of volcanic fields on Venus, Earth, and Mars: Lunar and Planetary Science, v. 32, p. 2179.

Lang, N.P., and Hansen, V.L., 2003, Geologic mapping of the Greenaway quadrangle (V24), Venus: Lunar and Planetary Science, v. 34, p. 1990.

Lecuyer, C., Simon, L., and Guyot, F., 2000, Comparison of carbon, nitrogen and water budgets on Venus and the Earth: Earth and Planetary Science Letters, v. 181, p. 33–40, doi: 10.1016/S0012-821X(00)00195-3.

López, I., and Hansen, V.L., 2003, Geologic mapping of the Helen Planitia quadrangle (V52), Venus: Lunar and Planetary Science, v. 34, p. 1061.

Mackwell, S.J., Zimmerman, M.E., and Kohlstedt, D.L., 1998, High-temperature deformation of dry diabase with application to tectonics on Venus: Journal of Geophysical Research, v. 103, p. 975–984, doi: 10.1029/97JB02671.

Masursky, H., Batson, R., Borgeson, W., Carr, M., McCauley, J., Milton, D., Wildey, R., Wilhelms, D., Murray, B., Horowitz, N., Leighton, R., Sharp, R., Thompson, W., Briggs, G., Chandeysson, P., Shipley, E., Sagan, C., Pollack, J., Lederberg, J., Levinthal, E., Hartmann, W., McCord, T., Smith, B., Davies, M., De Vaucouleurs, G., and Leovy, C., 1970, Television experiment for Mariner Mars 1971: Icarus, v. 12, p. 10–45, doi: 10.1016/0019-1035(70)90029-1.

Masursky, H., Eliason, E., Ford, P.G., McGill, G.E., Pettengill, G.H., Schaber, G.G., and Schubert, G., 1980, Pioneer Venus radar results: Geology from images and altimetry: Journal of Geophysical Research, v. 85, p. 8232–8260.

McGill, G.E., 2000, Geologic map of the Sappho Patera (V19) quadrangle, Venus: U.S. Geological Survey Geologic Investigations Series Map I-2637, scale 1:5,000,000.

McGill, G.E., 2004, Tectonic and stratigraphic implications of the relative ages of venusian plains and wrinkle ridges: Icarus, v. 172, p. 603–612.

McKinnon, W.B., Zahnle, K.J., Ivanov, B.A., and Melosh, H.J., 1997, Cratering on Venus: Models and observations, in Bouger, S.W., Hunten, D.M., and Phillips, R.J., eds., Venus II—Geology, geophysics, atmosphere, and solar wind environment: Tucson, University of Arizona Press, p. 969–1014.

Pettengill, G.H., Eliason, E., Ford, P.G., Loriot, G.B., Masursky, H., and McGill, G.E., 1980, Pioneer Venus radar results: Altimetry and surface properties: Journal of Geophysical Research, v. 85, p. 8261–8270.

Phillips, R.J., 1993, The age spectrum of the Venusian surface: Eos (Transactions, American Geophysical Union) (Supplement), v. 74, no. 16, p. 187.

Phillips, R.J., and Hansen, V.L., 1994, Tectonic and magmatic evolution of Venus: Annual Review of Earth and Planetary Science, v. 22, p. 597–654, doi: 10.1146/annurev.ea.22.050194.003121.

Phillips, R.J., and Hansen, V.L., 1998, Geological evolution of Venus: Rises, plains, plumes and plateaus: Science, v. 279, p. 1492–1497, doi: 10.1126/science.279.5356.1492.

Phillips, R.J., Raubertas, R.F., Arvidson, R.E., Sarkar, I.C., Herrick, R.R., Izenberg, N., and Grimm, R.E., 1992, Impact crater distribution and the resurfacing history of Venus: Journal of Geophysical Research, v. 97, p. 15,923–15,948.

Phillips, R.J., Bullock, M.A., and Hauck, S.A., II, 2001, Climate and interior coupled evolution on Venus: Geophysical Research Letters, v. 28, p. 1779–1782, doi: 10.1029/2000GL011821.

Reidel, S.P., and Hooper, P.R., eds., 1989, Volcanism and tectonism of the Columbia River flood basalt province: Geological Society of America Special Paper 239, p. 386.

Rosenberg, E., and McGill, G.E., 2001, Geologic map of the Pandrosos Dorsa (V5) quadrangle, Venus: U.S. Geological Survey Geologic Investigations Series Map I-2721, scale 1:5,000,000.

Sandwell, D.T., Johnson, C.L., and Suppe, J., 1997, Driving Forces for Limited Tectonics on Venus: Icarus, v. 129, p. 232–244.

Schaber, G.G., Strom, R.G., Moore, H.J., Soderblom, L.A., Kirk, R.L., Chadwick, D.J., Dawson, D.D., Gaddis, L.R., Boyce, J.M., and Russell, J., 1992, Geology and distribution of impact craters on Venus: What are they telling us?: Journal of Geophysical Research, v. 97, p. 13,257–13,302.

Schubert, G.S., Solomatov, V.S., Tackely, P.J., and Turcotte, D.L., 1997, Mantle convection and thermal evolution of Venus, in Bouger, S.W., Hunten, D.M., and Phillips, R.J., eds., Venus II—Geology, geophysics, atmosphere, and solar wind environment: Tucson, University of Arizona Press, p. 1245–1288.

Smrekar, S.E., Kiefer, W.S., and Stofan, E.R., 1997, Large volcanic rises on Venus, in Bouger, S.W., Hunten, D.M., and Phillips, R.J., eds., Venus II—Geology, geophysics, atmosphere, and solar wind environment: Tucson, University of Arizona Press, p. 845–879.

Snyder, D., 2002, Cooling of lava flows on Venus: The coupling of radiative and convective heat transfer: Journal of Geophysical Research, v. 107, p. 5080–5088, doi: 10.1029/2001JE001501.

Solomatov, V.S., and Moresi, L.N., 1996, Stagnant lid convection on Venus: Journal of Geophysical Research, v. 101, p. 4737–4753, doi: 10.1029/95JE03361.

Solomon, S.C., Bullock, M.A., and Grinspoon, D.H., 1999, Climate change as a regulator of tectonics on Venus: Science, v. 286, p. 87–90, doi: 10.1126/science.286.5437.87.

Stofan, E.R., Sharpton, V.L., Schubert, G., Baer, G., Bindschadler, D.L., Janes, D.M., and Squyres, S.W., 1992, Global distribution and characteristics of coronae and related features on Venus: Implications for origin and relation to mantle processes: Journal of Geophysical Research, v. 97, p. 13347–13378.

Stofan, E.R., Hamilton, V.E., Janes, D.M., and Smrekar, S.E., 1997, Coronae on Venus: Morphology and origin, in Bougher, S.W., Hunten, D.M., and Phillips, R.J., eds., Venus II—Geology, geophysics, atmosphere, and solar wind environment: Tucson, University of Arizona Press, p. 931–965.

Stofan, E.R., Anderson, S.W., Crown, D.A., and Plaut, J.J., 2000, Emplacement and composition of steep-sided domes on Venus: Journal of Geophysical Research, v. 105, p. 26757–26772, doi: 10.1029/1999JE001206.

Stofan, E.R., Smrekar, S.E., Tapper, S.W., Guest, J.E., and Grinrod, P.M., 2001, Preliminary analysis of an expanded corona data base for Venus: Geophysical Research Letters, v. 28, p. 4267–4270, doi: 10.1029/2001GL013307.

Strom, R.G., Schaber, G.G., and Dawson, D.D., 1994, The global resurfacing of Venus: Journal of Geophysical Research, v. 99, p. 10,899–10,926, doi: 10.1029/94JE00388.

Tanaka, K.T., Moore, H.J., Schaber, G.G., Chapman, M.G., Stofan, E.R., Campbell, D.B., Davis, P.A., Guest, J.E., McGill, G.E., Rogers, P.G., Saunders, R.S., and Zimbelman, J.R., 1994, The Venus geologic mappers' handbook: U.S. Geological Survey Open-File Report 94-438, 50 p.

Thompson, A.B., 2001, Partial melting of metavolcanics in amphibolite facies regional metamorphism: Proceedings of Indian Academy of Science, v. 110, p. 287–291.

Wilhelms, D.E., 1990, Geologic mapping, in Greeley, R., and Batson, R.M., eds., Planetary mapping: New York, Cambridge University Press, p. 208–260.

Young, D.A., and Hansen, V.L., 2003, Geologic map of the Rusalka quadrangle (V-25), Venus: U.S. Geological Survey Geologic Investigations Series Map I-2783, scale 1:5,000,000.

Zimbelman, J.R., 2001, Image resolution and evaluation of genetic hypotheses for planetary landscapes: Geomorphology, v. 37, p. 179–199, doi: 10.1016/S0169-555X(00)00082-9.

Zolotov, M.Y., Fegley, B., Jr., and Lodders, K., 1997, Hydrous silicates and water on Venus: Icarus, v. 130, p. 475–494, doi: 10.1006/icar.1997.5838.